Novel $Mn^{II}Mn^{III}Mn^{II}$ Trinuclear Complexes with Carbohydrate Bridges Derived from Seven-Coordinate Manganese(II) Complexes with *N*-Glycoside

Tomoaki Tanase,*,† Saori Tamakoshi,† Mayumi Doi,† Masahiro Mikuriya,‡ Hiromu Sakurai,§ and Shigenobu Yano*,†

Department of Chemistry, Faculty of Science, Nara Women's University, Nara-shi, Nara 630-8285, Japan, Department of Chemistry, School of Science, Kwansei Gakuin University, Nishinomiya-shi, Hyougo 662-8501, Japan, and Department of Analytical and Bioinorganic Chemistry, Kyoto Pharmaceutical University, Misasagi-Nakauchicho 5, Yamashina-ku, Kyoto 607-8414, Japan

Received March 30, 1999

Reactions of $MnX_2 \cdot nH_2O$ with tris(*N*-(D-mannosyl)-2-aminoethyl)amine ((D-Man)$_3$-tren), which was formed from D-mannose and tris(2-aminoethyl)amine (tren) in situ, afforded colorless crystals of $[Mn((D\text{-}Man)_3\text{-}tren)]X_2$ (**3a**, X = Cl; **3b**, X = Br; **3c**, X = NO_3; **3d**, X = $^1/_2SO_4$). The similar reaction of $MnSO_4 \cdot 5H_2O$ with tris(*N*-(L-rhamnosyl)-2-aminoethyl)amine ((L-Rha)$_3$-tren) gave $[Mn((L\text{-}Rha)_3\text{-}tren)]SO_4$ (**4d**), where L-rhamnose is 6-deoxy-L-mannose. The structures of **3b** and **4d** were determined by X-ray crystallography to have a seven-coordinate Mn(II) center ligated by the *N*-glycoside ligand, (aldose)$_3$-tren, with a C_3 helical structure. Three D-mannosyl residues of **3b** are arranged in a $\Delta(ob_3)$ configuration around the metal, leading to formation of a cage-type sugar domain in which a water molecule is trapped. In **4d**, three L-rhamnosyl moieties are in a $\Delta(lel_3)$ configuration to form a facially opened sugar domain on which a sulfate anion is capping through hydrogen bonding. These structures demonstrated that a configurational switch around the seven-coordinate manganese(II) center occurs depending on its counteranion. Reactions of **3a**, **3b**, and **4d** with 0.5 equiv of Mn(II) salt in the presence of triethylamine yielded reddish orange crystals formulated as $[\{Mn((aldose)_3\text{-}tren)\}_2Mn(H_2O)]X_3 \cdot nH_2O$ (**5a**, aldose = D-Man, X = Cl; **5b**, aldose = D-Man, X = Br; **6d**, aldose = L-Rha, X = $^1/_2SO_4$). The analogous trinuclear complexes **6a** (aldose = L-Rha, X = Cl), **6b** (aldose = L-Rha, X = Br), and **6c** (aldose = L-Rha, X = NO_3) were prepared by the one-pot reaction of Mn(II) salts with (L-Rha)$_3$-tren without isolation of the intermediate Mn(II) complexes. X-ray crystallographic studies revealed that **5a**, **5b**, **6c**, and **6d** have a linearly ordered trimanganese core, $Mn^{II}Mn^{III}Mn^{II}$, bridged by two carbohydrate residues with Mn−Mn separations of 3.845(2)−3.919(4) Å and Mn−Mn−Mn angles of 170.7(1)−173.81(7)°. The terminal Mn(II) atoms are seven-coordinate with a distorted mono-face-capped octahedral geometry ligated by the (aldose)$_3$-tren ligand through three oxygen atoms of C-2 hydroxyl groups, three N-glycosidic nitrogen atoms, and a tertiary amino group. The central Mn(III) atoms are five-coordinate ligated by four oxygen atoms of carbohydrate residues in the (aldose)$_3$-tren ligands and one water molecule, resulting in a square-pyramidal geometry. In the bridging part, a β-aldopyranosyl unit with a chair conformation bridges the two $Mn^{II}Mn^{III}$ ions with the C-2 μ-alkoxo group and with the C-1 N-glycosidic amino and the C-3 alkoxo groups coordinating to each metal center. These structures could be very useful information in relation to xylose isomerases which promote aldose−ketose isomerization by using divalent dimetal centers such as Mn^{2+}, Mg^{2+}, and Co^{2+}.

Introduction

Carbohydrates are indispensable building blocks and energy sources to living organisms and play important roles in many biological functions.[1] Studies on interactions of carbohydrates with metal ions have become one of the most important subjects in the bioinorganic field, since many sugar-metabolizing enzymes have been revealed to function with metal ions such as Mg^{2+}, Mn^{2+}, Co^{2+}, and Zn^{2+} in the active sites.[2−6] Bioinorganic chemistry with sugars, however, is largely unexplored in comparison with that with amino acids and nucleic acids,[7] owing mainly to their multifunctionality, hygroscopic nature, complicated stereochemistry, and relatively low coordination ability to metal ions. Recent biological studies have notably shown the importance of dinuclear metal aggregations, in particular with Mn^{2+} and Mg^{2+} ions, in some enzymes and

† Nara Women's University.
‡ Kwansei Gakuin University.
§ Kyoto Pharmaceutical University.

(1) Kennedy, J. F.; White, C. A. *Bioactive Carbohydrates in Chemistry, Biochemistry and Biology*; John Wiley & Sons: New York, 1983.
(2) (a) Gracy, R. W.; Noltmann, E. A. *J. Biol. Chem.* **1968**, *243*, 4109. (b) Gracy, R. W.; Noltmann, E. A. *J. Biol. Chem.* **1968**, *243*, 5410.
(3) Root, R. L.; Durrwachter, J. R.; Wong, C.-H. *J. Am. Chem. Soc.* **1985**, *107*, 2997.
(4) (a) Jenkins, J.; Janin, J.; Rey, F.; Chiadmi, M.; Tilbeurgh, H.; Lasters, I.; Maeyer, M. D.; Belle, D. V.; Wodak, S. J.; Lauwereys, M.; Stanssens, P.; Mrabet, N. T.; Snauwaert, J.; Matthyssens, G.; Lambeir, A.-M. *Biochemistry* **1992**, *31*, 5449. (b) Whitlow, M.; Howard, A. J.; Finzel, B. C.; Poulos, T. L.; Winborne, E.; Gilliland, G. L. *Proteins* **1991**, *9*, 153.
(5) (a) Zhang, Y.; Liang, J.-Y.; Huang, S.; Ke, H.; Lipscomb, W. N. *Biochemistry* **1993**, *32*, 17. (b) Xue, Y.; Huang, S.; Liang, J.-Y.; Zhang, Y.; Lipscomb, W. N. *Proc. Natl. Acad. Sci. U.S.A.* **1994**, *91*, 12482.
(6) Hardman, K. D.; Agarwal, R. C.; Freiser, M. *J. Mol. Biol.* **1982**, *157*, 69.
(7) (a) Angyal, S. J. *Chem. Soc. Rev.* **1980**, *9*, 415. (b) Angyal, S. J. *Adv. Carbohydr. Chem. Biochem.* **1989**, *47*, 1. (c) Whitfield, D. M.; Stojkovski, S.; Sarkar, B. *Coord. Chem. Rev.* **1993**, *122*, 171.

10.1021/ic990349r CCC: $19.00
Published on Web 01/27/2000

proteins handling sugar derivatives. Xylose isomerases promote aldose−ketose isomerization by utilizing a carboxylate-bridged dimetal center of Mg^{2+}, Mn^{2+}, or Co^{2+} ions in the active site ~4.9 Å apart.[4] The similar dinuclear array of Mg^{2+} or Mn^{2+} in ~3.7 Å separation also promotes the cleavage of phosphate esters in fructose 1,6-bisphosphatase.[5] Concanavalin A, a lectin which specifically binds saccharides containing mannosyl residues, involves a pair of Ca^{2+} and Mn^{2+} ions bridged by an aspartate.[6]

We have studied the chemistry of transition-metal complexes with carbohydrates utilizing N-glycosidic bond formation[8] and recently reported the synthesis and characterization of seven-coordinate cobalt(II) complexes, $[Co((D\text{-}Man)_3\text{-tren})]X_2$ (**1a**, X = Cl; **1b**, X = Br; **1d**, X = $^1/_2SO_4$) and $[Co((L\text{-}Rha)_3\text{-tren})]X_2$ (**2a**, X = Cl; **2b**, X = Br; **2d**, X = $^1/_2SO_4$)[9] with a cage-type heptadentate *N*-glycoside ligand, tris((*N*-aldosyl)-2-aminoethyl)-amine, from tris(2-aminoethyl)amine (tren) and D-mannose (D-Man) or L-rhamnose (L-Rha = 6-deoxy-L-mannose). Complexes **1** and **2** showed a dynamic chiral inversion around the metal center which was induced by the interaction of sugars with the SO_4^{2-} anion; e.g., $[Co((L\text{-}Rha)_3\text{-tren})]Br_2$ (**2b**) adopts a Λ-C_3-helical configuration and $[Co((L\text{-}Rha)_3\text{-tren})]SO_4$ (**2d**) takes a Δ-C_3-helical configuration, both of which were determined by X-ray crystallographic analyses. The interconversion from Λ to Δ through capturing a sulfate anion into the sugar pocket could be regarded as a potential model for the induced-fit observed in biological systems, and thus, the effort to expand this system by using other biological metal ions such as Mn^{2+} is valuable. Here, we report the synthesis of mononuclear manganese(II) complexes of the heptadentate *N*-glycoside ligand which were converted into novel trimanganese complexes with a linear $Mn^{II}Mn^{III}Mn^{II}$ core bridged by an equatorial−axial−equatorial donor sequence of β-mannopyranosyl moieties. Preliminary accounts have already been reported.[10]

Experimental Section

Materials. All reagents were of the best commercial grade and were used as received. The following abbreviations are used: tren, tris(2-aminoethyl)amine; D-Man, D-mannose; L-Rha, L-rhamnose (6-deoxy-L-mannose); *N*,*N*′,*N*″-(aldose)$_3$-tren, tris(*N*-aldosyl-2-aminoethyl)amine. All experiments were carried out under aerobic conditions.

Measurements. Electronic absorption spectra were recorded on a Jasco UV570 spectrometer and circular dichroism spectra on a Jasco J-720 spectropolarimeter. IR spectra were measured on KBr pellets with a Jasco FT/IR-8900μ spectrometer. Magnetic susceptibilities at room temperature were measured by the Gouy method with a Sherwood MSB-MKI magnetic balance. The diamagnetism of the complexes was corrected from Pascal's constants.[11] Variable-temperature magnetic susceptibility data were measured over a range of 4−300 K by a Quantum Design model MPMS-5S superconducting quantum interference device (SQUID). Electron paramagnetic resonance (EPR) spectra of methanolic solution samples were obtained using a JEOL JES FE-3XG spectrometer equipped with a digital frequency counter, Advantest TR-5212, at 298 and 77 K.

Preparations of $[Mn((D\text{-}Man)_3\text{-tren})]X_2$ (X = Cl (3a), Br (3b), NO_3 (3c), $^1/_2SO_4$ (3d)) and $[Mn((L\text{-}Rha)_3\text{-tren})]SO_4$ (4d)). Method A. A methanolic solution (100 mL) containing tren (0.44 g, 3.0 mmol) and D-mannose (2.16 g, 12.0 mmol) was incubated at 50−55 °C for 3 h. To the resultant pale yellow solution was added a methanolic solution (20 mL) of $MnCl_2\cdot 4H_2O$ (0.59 g, 3.0 mmol). The reaction mixture was further heated at 55−60 °C for 1 h, and then, the reddish-orange reaction solution was allowed to stand at room temperature for 12 h. The concentrated reaction solution was loaded onto a Sephadex LH-20 GPC column (80 cm × 4 cm o.d.) eluted with methanol. The pale pink main band was collected and concentrated by a rotary evaporator to ca. 25 mL, affording colorless hexagonal prismatic crystals of **3a**·$5H_2O$, $[Mn((D\text{-}Man)_3\text{-tren})]Cl_2\cdot 5H_2O$. The crystals were collected and dried in a vacuum (yield 27% based on Mn). Anal. Calcd for $C_{24}H_{58}N_4O_{20}MnCl_2$: C, 33.97: H, 6.89; N, 6.60; Cl, 8.36. Found: C, 33.99; H, 6.80; N, 6.76; Cl, 8.41. μ_{eff} (rt) = 5.63 μ_B. IR (KBr): 3258br, 1627m, 1453, 1408m, 1375, 1306, 1237, 1142, 1105, 1083s, 1028, 961, 911, 879, 858, 793, 733, 669 cm^{-1}.

A similar procedure with $MnBr_2\cdot 4H_2O$ gave colorless hexagonal prismatic crystals of **3b**·$4H_2O$, $[Mn((D\text{-}Man)_3\text{-tren})]Br_2\cdot 4H_2O$ (yield 58% vs Mn). Anal. Calcd for $C_{24}H_{56}N_4O_{19}MnBr_2$: C, 31.35: H, 6.14; N, 6.09; Br, 17.38; Mn, 5.97. Found: C, 31.00; H, 6.37; N, 5.93; Br, 17.46; Mn, 6.05. μ_{eff} (rt) = 5.62 μ_B. IR (KBr): 3356br, 1628m, 1453, 1406m, 1306, 1238, 1105, 1082s, 961, 911, 881, 857, 792m, 673, 622 cm^{-1}.

A methanolic solution (100 mL) containing tren (0.44 g, 3.0 mmol) and D-mannose (2.16 g, 12.0 mmol) was incubated at 50−55 °C for 3 h. To the resultant pale yellow solution was added a methanolic solution (20 mL) of $Mn(NO_3)_2\cdot 6H_2O$ (0.86 g, 3.0 mmol). The reaction mixture was further heated at 50−55 °C for 1 h, and then, the reddish-orange reaction solution was allowed to stand at room temperature for 12 h to give colorless crystals of **3c**·$4H_2O$, $[Mn((D\text{-}Man)_3\text{-tren})](NO_3)_2\cdot 4H_2O$ (yield 33% vs Mn). Anal. Calcd for $C_{24}H_{56}N_6O_{25}Mn$: C, 32.62: H, 6.39; N, 9.51; Mn, 6.22. Found: C, 32.92; H, 6.34; N, 9.49; Mn, 6.35. μ_{eff} (rt) = 5.62 μ_B. IR (KBr): 3406br, 1652m, 1383s, 1090s, 912, 790, 719, 621 cm^{-1}.

To the methanolic solution containing tris(*N*-(D-mannosyl)-2-aminoethyl)amine mentioned above was added powdered $MnSO_4\cdot 5H_2O$ (0.72 g, 3.0 mmol). The solution was further heated at 50−55 °C for 1 h and, then, allowed to stand at room temperature for 12 h to give colorless microcrystals of **3d**·$4H_2O$, $[Mn((D\text{-}Man)_3\text{-tren})]SO_4\cdot 4H_2O$ (yield 82% vs Mn). Anal. Calcd for $C_{24}H_{56}N_4O_{23}MnS$: C, 33.69: H, 6.60; N, 6.55; Mn, 6.42. Found: C, 33.52; H, 6.67; N, 6.46; Mn, 6.94. μ_{eff} (rt) = 5.89 μ_B. IR (KBr): 3358br, 1650m, 1457, 1355, 1305, 1188, 1099s, 961, 909, 790, 709 cm^{-1}.

A methanolic solution (100 mL) containing tren (0.44 g, 3.0 mmol) and L-rhamnose monohydrate (2.19 g, 12.0 mmol) was incubated at 50−55 °C for 3 h. To the resultant solution was added powdered $MnSO_4\cdot 5H_2O$ (0.72 g, 3.0 mmol). The mixture was heated at 50−55

(8) (a) Yano, S. *Coord. Chem. Rev.* **1988**, *92*, 113 and references therein. (b) Yano, S.; Ohtsuka, M. In *Metal Ions in Biological Systems*; Sigel, H., Sigel A. Eds.; Marcel Dekker: New York, 1995; Vol. 32, p 27. (c) Ishida, K.; Nonoyama, S.; Hirano, T.; Yano, S.; Hidai, M.; Yoshikawa, S. *J. Am. Chem. Soc.* **1989**, *111*, 1599. (d) Ishida, K.; Yashiro, M.; Yano, S.; Hidai, M.; Yoshikawa, S. *J. Chem. Soc., Dalton Trans.* **1989**, 1241. (e) Takei, T.; Tanase, T.; Yano, S.; Hidai, M. *Chem. Lett.* **1991**, 1629. (f) Tanase, T.; Takei, T.; Hidai, M.; Yano, S. *J. Chem. Res., Synop.* **1992**, 252; *J. Chem. Res., Miniprint* 1922. (g) Tanase, T.; Nouchi, R.; Oka, Y.; Kato, M.; Nakamura, N.; Yamamura, T.; Yamamoto, Y.; Yano, S. *J. Chem. Soc., Dalton Trans.* **1993**, 2645. (h) Yano, S.; Kato, M.; Shioi, H.; Takahashi, T.; Tsubomura, T.; Toriumi, K.; Ito, T.; Hidai, M.; Yoshikawa, S. *J. Chem. Soc., Dalton Trans.* **1993**, 1699. (i) Yano, S.; Doi, M.; Kato, M.; Okura, I.; Nagano, T.; Yamamoto, Y.; Tanase, T. *Inorg. Chim. Acta* **1996**, *249*, 1. (j) Tanase, T.; Nouchi, R.; Doi, M.; Kato, M.; Sato, Y.; Ishida, K.; Kobayashi, K.; Sakurai, T.; Yamamoto, Y.; Yano, S. *Inorg. Chem.* **1996**, *35*, 4848. (k) Tanase, T.; Onaka, T.; Nakagoshi, M.; Kinoshita, I.; Shibata, K.; Doe, M.; Fujii, J.; Yano, S. *Chem. Commun.* **1997**, 2115. (l) Yano, S.; Inoue, S.; Nouchi, R.; Mogami, K.; Shinohara, Y.; Yasuda, Y.; Kato, M.; Tanase, T.; Kakuchi, T.; Mikata, Y.; Suzuki, T.; Yamamoto, Y. *J. Inorg. Biochem.* **1998**, *69*, 15. (m) Tanase, T.; Yasuda, Y.; Onaka, T.; Yano, S. *J. Chem. Soc., Dalton Trans.* **1998**, 345.

(9) (a) Tanase, T.; Nakagoshi, M.; Teratani, A.; Kato, M.; Yamamoto, Y.; Yano, S. *Inorg. Chem.* **1994**, *33*, 6. (b) Yano, S.; Nakagoshi, M.; Teratani, A.; Kato, M.; Tanase, T.; Yamamoto, Y.; Uekusa, H.; Ohashi, Y. *Mol. Cryst. Liq. Cryst.* **1996**, *276*, 253. (c) Yano, S.; Nakagoshi, M.; Teratani, A.; Kato, M.; Onaka, T.; Iida, M.; Tanase, T.; Yamamoto, Y.; Uekusa, H.; Ohashi, Y. *Inorg. Chem.* **1997**, *36*, 4187.

(10) (a) Yano, S.; Doi, M.; Tamakoshi, S.; Mori, W.; Mikuriya, M.; Ichikawa, A.; Kinoshita, I.; Yamamoto, Y.; Tanase, T. *Chem. Commun.* **1997**, 997. (b) Tanase, T.; Tamakoshi, S.; Doi, M.; Mori, W.; Yano, S. *Inorg. Chim. Acta* **1997**, *266*, 5.

(11) (a) Figgs, B. N.; Lewis, J. In *Modern Coordination Chemistry*; Lewis, J., Wilkins, R. G., Eds.; Interscience: New York, 1960. (b) O'Connor, C. J. *Prog. Inorg. Chem.* **1982**, *29*, 203. (c) Mabbs, F. E.; Machin, D. J. *Magnetism and Transition Metal Complexes*; Chapman and Hall: London, 1973.

Table 1. Crystallographic and Experimental Data for $[Mn((D\text{-}Man)_3\text{-tren})]Br_2\cdot 3.5H_2O$ (**3b**·3.5H_2O) and $[Mn((L\text{-}Rha)_3\text{-tren})]SO_4\cdot 4CH_3OH$ (**4d**)

	3b·3.5H_2O	**4d**·4CH_3OH
formula	$C_{24}H_{55}N_4O_{18.5}MnBr_2$	$C_{28}H_{64}N_4O_{20}MnS$
fw	910.46	863.83
cryst syst	trigonal	orthorhombic
space group	$P321$ (No. 150)	$P2_12_12_1$ (No. 19)
a, Å	11.092(3)	13.526(5)
b, Å		23.765(4)
c, Å	17.955(3)	12.104(4)
V, Å^3	1913(1)	3890(1)
Z	2	4
T, °C	−99	−100
D_{calcd}, g cm^{-1}	1.580	1.475
abs coeff, cm^{-1}	25.16	4.77
2θ range, deg	$3 < 2\theta < 56$	$3 < 2\theta < 50$
instrument	Rigaku AFC7R	Rigaku AFC5S
solution	direct methods (SIR92)	direct methods (SIR92)
no. of unique data	1784	3864
no. of obsd data	1267 ($I > 3\sigma(I)$)	2342 ($I > 2\sigma(I)$)
no. of variables	161	328
p-factor	0.03	0.03
R^a	0.059	0.085
$R_w{}^a$	0.061	0.087
GOF^b	2.33	2.04

^{a} $R = \sum||F_o| - |F_c||/\sum|F_o|$; $R_w = [\sum w(|F_o| - |F_c|)^2/\sum w|F_o|^2]^{1/2}$ ($w = 1/\sigma^2(F_o)$). ^{b} GOF $= [\sum w(|F_o| - |F_c|)^2/(N_o - N_p)]^{1/2}$ (N_o = no. of data, N_p = no. of variables).

°C for 1 h and, then, allowed to stand at room temperature for 12 h. The concentrated reaction solution was loaded onto a Sephadex LH-20 GPC column (80 cm × 4 cm o.d.) eluted with methanol. The pale pink main band was collected and concentrated by a rotary evaporator to ca. 30 mL, affording colorless prismatic crystals of **4d**·4H_2O, $[Mn((L\text{-}Rha)_3\text{-tren})]SO_4\cdot 4H_2O$ (yield 42% vs Mn). Anal. Calcd for $C_{24}H_{56}N_4O_{20}SMn$: C, 35.69: H, 6.99; N, 6.94; Mn, 6.80. Found: C, 35.87; H, 6.88; N, 7.02; Mn, 6.70. μ_{eff} (rt) = 5.83 μ_B. IR (KBr): 3375br, 1653m, 1456, 1374, 1351, 1314, 1291, 1190, 1097s, 966, 900, 880, 850, 784, 711, 621 cm^{-1}.

Preparations of $[\{Mn((D\text{-}Man)_3\text{-tren})\}_2Mn(H_2O)]X_3$ (X = Cl (5a), Br (5b)) and $[\{Mn((L\text{-}Rha)_3\text{-tren})\}_2Mn(H_2O)]X_3$ (X = Cl (6a), Br (6b), NO_3 (6c), $^1/_2SO_4$ (6d)). Method B. Complex **3a**·5H_2O, $[Mn((D\text{-}Man)_3\text{-tren})]Cl_2\cdot 5H_2O$ (300 mg, 0.35 mmol) was dissolved in methanol (50 mL) at 60 °C. After the solution was cooled to room temperature, $MnCl_2\cdot 4H_2O$ (35 mg, 0.18 mmol) was added and the solution was stirred at room temperature for 30 min. Then, about 50 mg of triethylamine was added to the solution, which was further stirred at room temperature for 12 h in air. The color of the solution changed from colorless to reddish orange. The concentrated reaction solution was loaded onto a Sephadex LH-20 GPC column (80 cm × 4 cm o.d.) eluted with methanol. The reddish orange main band was collected and concentrated by a rotary evaporator to ca. 5 mL. Vapor diffusion of EtOH into the concentrated solution in a refrigerator afforded trigonal prismatic orange crystals of **5a**·6.5H_2O, $[\{Mn((D\text{-}Man)_3\text{-tren})\}_2Mn(H_2O)]Cl_3\cdot 6.5H_2O$, which were collected and dried in a vacuum (yield 20% vs **1**·5H_2O). Anal. Calcd for $C_{48}H_{107}N_8O_{37.5}Cl_3Mn_3$: C, 34.57; H, 6.47; N, 6.72; Cl, 6.38. Found: C, 34.08; H, 5.91; N, 6.70; Cl, 6.37. μ_{eff} (rt) = 9.03 μ_B. UV−vis (in CH_3OH): ν_{max} (ϵ) 20.49 (418) $10^3 \times$ cm^{-1} (M^{-1} cm^{-1}). CD (in CH_3OH): ν_{max} ($\Delta\epsilon$) 19.19 (−1.08), 22.94 (−0.72), 32.57 (+3.18) $10^3 \times$ cm^{-1} (M^{-1} cm^{-1}). IR (KBr): 3364br, 1645m, 1465, 1373, 1288, 1191, 1067s, 960, 910, 802, 753, 710 cm^{-1}.

Similar procedures (method B) using **3b**·4H_2O (100 mg, 0.11 mmol)/$MnBr_2\cdot 4H_2O$ (16 mg, 0.055 mmol) and **4d**·4H_2O (100 mg, 0.12 mmol)/$MnSO_4\cdot 5H_2O$ (15 mg, 0.062 mmol) as starting metal sources afforded reddish orange crystals of **5b**·4H_2O, $[\{Mn((D\text{-}Man)_3\text{-tren})\}_2Mn(H_2O)]Br_3\cdot 4H_2O$ (26% vs **3b**·4H_2O), and **6d**·7H_2O, $[\{Mn((L\text{-}Rha)_3\text{-tren})\}_2Mn(H_2O)](SO_4)_{1.5}\cdot 7H_2O$ (19% vs **4d**·4H_2O). For **5b**·4H_2O: Anal. Calcd for $C_{48}H_{102}N_8O_{35}Br_3Mn_3$: C, 32.83; H, 5.86; N, 6.38; Br, 13.65. Found: C, 32.93; H, 5.85; N, 6.28; Br, 13.75. μ_{eff} (rt) = 8.86 μ_B. UV−vis (in CH_3OH): ν_{max} (ϵ) 20.83 (266) $10^3 \times$ cm^{-1} (M^{-1} cm^{-1}). CD (in CH_3OH): ν_{max} ($\Delta\epsilon$) 19.55 (−0.58), 23.28 (−0.49), 31.55 (+1.53) $10^3 \times$ cm^{-1} (M^{-1} cm^{-1}). IR (KBr): 3379br, 1638m, 1466, 1374, 1286, 1191, 1066s, 958, 909, 802, 753, 710 cm^{-1}. For **6d**·7H_2O: Anal. Calcd for $C_{48}H_{108}N_8O_{38}S_{1.5}Mn_3$: C, 35.62; H, 6.73; N, 6.92; S, 2.97. Found: C, 35.74; H, 6.97; N, 6.57; S, 2.74. μ_{eff} (rt) = 8.46 μ_B. UV−vis (in CH_3OH): ν_{max} (ϵ) 19.84 (604) $10^3 \times$ cm^{-1} (M^{-1} cm^{-1}). CD (in CH_3OH): ν_{max} ($\Delta\epsilon$) 19.07 (+1.14), 23.47 (+1.32), 32.68 (−3.46) $10^3 \times$ cm^{-1} (M^{-1} cm^{-1}). IR (KBr): 3394br, 1645m, 1451, 1376, 1352, 1289, 1192, 1116s, 970, 902, 882, 846, 804, 751, 709, 618 cm^{-1}.

Table 2. Crystallographic and Experimental Data

(a) $[\{Mn((D\text{-}Man)_3\text{-tren})\}Mn(H_2O)]Cl_3\cdot 6H_2O$ (**5a**·6H_2O) and $[\{Mn((D\text{-}Man)_3\text{-tren})\}Mn(H_2O)]Br_3\cdot 8H_2O$ (**5b**·8H_2O)

compound	**5a**·6H_2O	**5b**·8H_2O
formula	$C_{48}H_{106}N_8O_{37}Mn_3Cl_3$	$C_{48}H_{116}N_8O_{39}Mn_3Br_3$
fw	1658.57	1834.00
cryst syst	trigonal	trigonal
space group	$P3_1$ (No. 144)	$P3_1$ (No. 144)
a, Å	12.712(8)	12.857(4)
c, Å	41.053(9)	40.961(9)
V, Å^3	5744(6)	5863(1)
Z	3	3
T, °C	−147	−99
D_{calcd}, g cm^{-1}	1.438	1.558
abs coeff, cm^{-1}	6.82	21.08
2θ range, deg	$3 < 2\theta < 45$	$3 < 2\theta < 50$
instrument	Rigaku AFC5S	Rigaku AFC7R
solution	direct methods (SIR92)	direct methods (SIR92)
no. of unique data	5073	6857
no. of obsd data	3108 ($I > 3\sigma(I)$)	3808 ($I > 3\sigma(I)$)
no. of variables	652	639
p-factor	0.03	0.03
R^a	0.083	0.081
$R_w{}^a$	0.091	0.085
GOF^b	2.43	2.68

(b) $[\{Mn((L\text{-}Rha)_3\text{-tren})\}Mn(H_2O)](NO_3)_3\cdot 5H_2O$ (**6c**·5H_2O) and $[\{Mn((L\text{-}Rha)_3\text{-tren})\}Mn(H_2O)](SO_4)_{1.5}\cdot 10H_2O$ (**6d**·10H_2O)

compound	**6c**·5H_2O	**6d**·10H_2O
formula	$C_{48}H_{104}N_{11}O_{39}Mn_3$	$C_{48}H_{114}N_8O_{41}Mn_3S_{1.5}$
fw	1624.21	1672.36
cryst syst	orthorhombic	orthorhombic
space group	$C222_1$ (No. 20)	$C222_1$ (No. 20)
a, Å	12.925(5)	12.908(4)
b, Å	21.255(7)	21.818(6)
c, Å	26.871(8)	27.693(8)
V, Å^3	7382(3)	7799(3)
Z	4	4
T, °C	−147	−98
D_{calcd}, g cm^{-1}	1.461	1.424
abs coeff, cm^{-1}	6.04	6.14
2θ range, deg	$3 < 2\theta < 50$	$3 < 2\theta < 50$
instrument	Rigaku AFC5S	Rigaku AFC7R
solution	direct methods (SIR92)	direct methods (SIR92)
no. of unique data	3598	3796
no. of obsd data	2319 ($I > 3\sigma(I)$)	3106 ($I > 3\sigma(I)$)
no. of variables	321	449
p-factor	0.03	0.03
R^a	0.073	0.061
$R_w{}^a$	0.073	0.073
GOF^b	2.09	2.80

^{a} $R = \sum||F_o| - |F_c||/\sum|F_o|$; $R_w = [\sum w(|F_o| - |F_c|)^2/\sum w|F_o|^2]^{1/2}$ ($w = 1/\sigma^2(F_o)$). ^{b} GOF $= [\sum w(|F_o| - |F_c|)^2/(N_o - N_p)]^{1/2}$ (N_o = no. of data, N_p = no. of variables).

Method A. A methanolic solution (100 mL) containing tren (0.44 g, 3.0 mmol) and L-Rha·H_2O (2.19 g, 12.0 mmol) was incubated at 50−55 °C for 3 h. To the resultant pale yellow solution was added $MnCl_2\cdot 4H_2O$ (0.59 g, 3.0 mmol). The reddish-orange reaction solution was heated at 50−55 °C for 1 h and, then, allowed to stand at room temperature for 12 h in air. The concentrated solution was chromatographed on a Sephadex LH-20 GPC column (80 cm × 4 cm o.d.) eluted with methanol. The reddish-orange main band was collected and slowly evaporated at room temperature to afford reddish-orange needle crystals

Scheme 1[a]

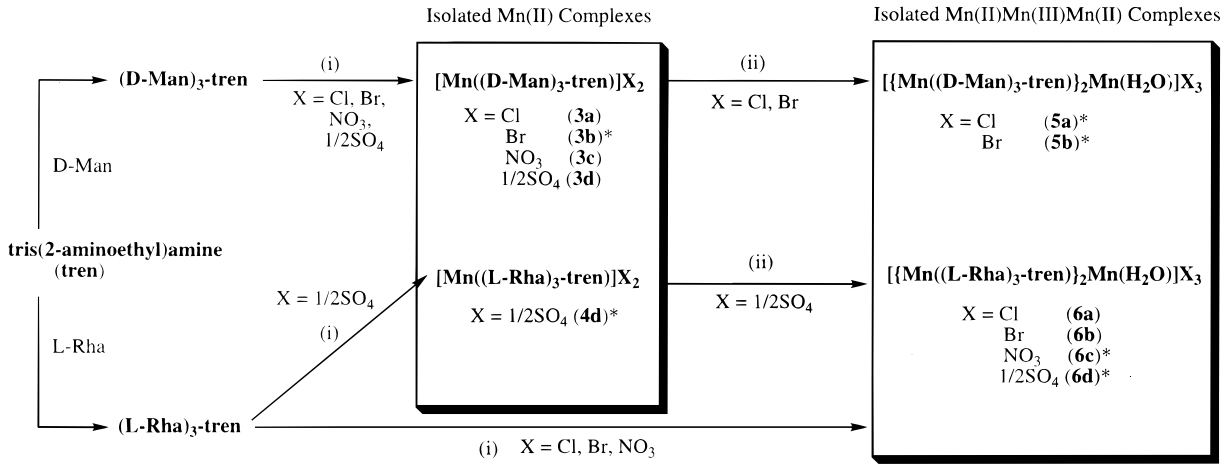

[a] (i) Treated with $MnX_2 \cdot nH_2O$ (1 equiv) in MeOH at 50−55 °C for 1 h (method A). (ii) Treated with $MnX_2 \cdot nH_2O$ (0.5 equiv) in the presence of Et_3N in MeOH at room temperature for 12 h (method B). *Characterized by X-ray crystallography.

Scheme 2

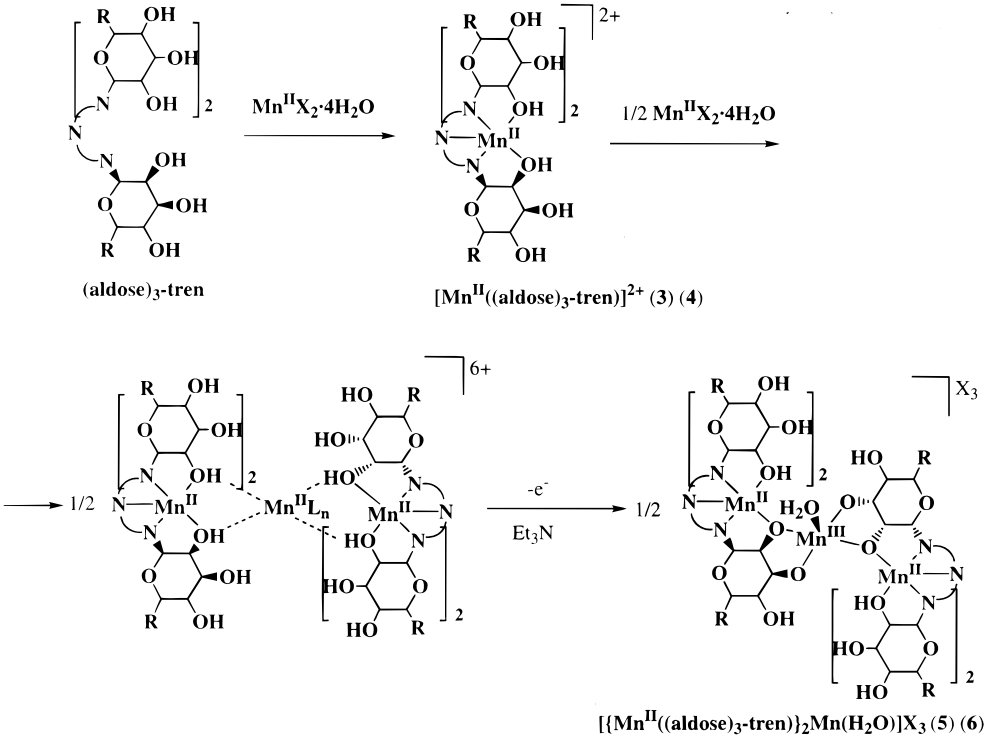

of **6a**·$11H_2O$, [{Mn((L-Rha)$_3$-tren)}$_2$Mn(H_2O)]Cl_3·$11H_2O$. The crystals were collected and dried in a vacuum (yield 43% vs Mn). Complexes **6b**·$10H_2O$, [{Mn((L-Rha)$_3$-tren)}$_2$Mn(H_2O)]Br_3·$10H_2O$ (yield 31%), and **6c**·$8H_2O$, [{Mn((L-Rha)$_3$-tren)}$_2$Mn(H_2O)]$(NO_3)_3$·$8H_2O$ (yield 42%), were prepared by similar procedures by using $MnBr_2$·$4H_2O$ and $Mn(NO_3)_2$·$6H_2O$, respectively. For **6a**·$11H_2O$: Anal. Calcd for $C_{48}H_{116}N_8O_{36}Cl_3Mn_3$: C, 34.88; H, 7.07; N, 6.78; Cl, 6.44; Mn, 9.97. Found: C, 34.97; H, 6.62; N, 6.73; Cl, 6.93; Mn, 8.63. μ_{eff} (rt) = 9.12 μ_B. UV−vis (in CH_3OH): ν_{max} (ϵ) 20.41(482) $10^3 \times cm^{-1}$ (M^{-1} cm^{-1}). CD (in CH_3OH): ν_{max} ($\Delta\epsilon$) 18.94 (+1.12), 23.15 (+0.68), 33.00 (−2.60) $10^3 \times cm^{-1}$ (M^{-1} cm^{-1}). IR (KBr): 3382br, 1647m, 1456, 1375, 1192, 1068s, 969, 901, 804, 748, 707 cm^{-1}. For **6b**·$10H_2O$: Anal. Calcd for $C_{48}H_{114}N_8O_{35}Br_3Mn_3$: C, 32.61; H, 6.50; N, 6.34; Br, 13.56; Mn, 9.32. Found: C, 32.61; H, 6.03; N, 6.29; Br, 13.72; Mn, 8.64. μ_{eff} (rt) = 9.28 μ_B. UV−vis (in CH_3OH): ν_{max} (ϵ) 20.53(518) $10^3 \times cm^{-1}$ (M^{-1} cm^{-1}). CD (in CH_3OH): ν_{max} ($\Delta\epsilon$) 19.34 (+1.32), 23.31 (+1.11), 31.15 (−2.81) $10^3 \times cm^{-1}$ (M^{-1} cm^{-1}). IR (KBr): 3367br, 1652, 1456, 1378, 1286, 1192, 1084s, 967, 901, 805, 755, 709 cm^{-1}. For **6c**·$8H_2O$: Anal. Calcd for $C_{48}H_{110}N_{11}O_{42}Mn_3$: C, 34.35; H, 6.61; N, 9.18; Mn, 9.82. Found: C, 34.21; H, 6.29; N, 9.39; Mn, 7.99. μ_{eff} (rt) = 8.88 μ_B. UV−vis (in CH_3OH): ν_{max} (ϵ) 21.19 (437) $10^3 \times cm^{-1}$ (M^{-1} cm^{-1}). CD (in CH_3OH): ν_{max} ($\Delta\epsilon$) 20.24 (+1.09), 32.47 (−2.46) $10^3 \times cm^{-1}$ (M^{-1} cm^{-1}). IR (KBr): 3365br, 1655m, 1384s, 1192, 1067s, 972, 901, 803, 752, 713 cm^{-1}.

X-ray Crystallography. Crystals of **3b**·$3.5H_2O$, **4d**·$4CH_3OH$, **5a**·$6H_2O$, **5b**·$8H_2O$, **6c**·$5H_2O$, and **6d**·$10H_2O$ were suitable for X-ray crystallography although they were extremely delicate when they were separated from the mother liquors. The crystals of **3b**, **4d**, **5a**, **5b**, and **6d** were quickly coated with Paraton N oil (Exxon) and were mounted on the top of glass fiber at low temperature, and the crystal of **6c** was sealed into a glass tube capillary with a droplet of its mother liquor. Crystal data and experimental conditions are summarized in Tables 1 and 2. All data were collected at −98 to −99 °C (**3b**, **5b**, **6d**) on Rigaku AFC7R and at −100 °C (**4d**), −147 °C (**5a**), and 23 °C (**6c**) on Rigaku AFC5S diffractometers equipped with graphite-monochromatized Mo Kα (λ = 0.710 69 Å) radiation. Three standard reflections were monitored every 150 reflections and showed no systematic decrease

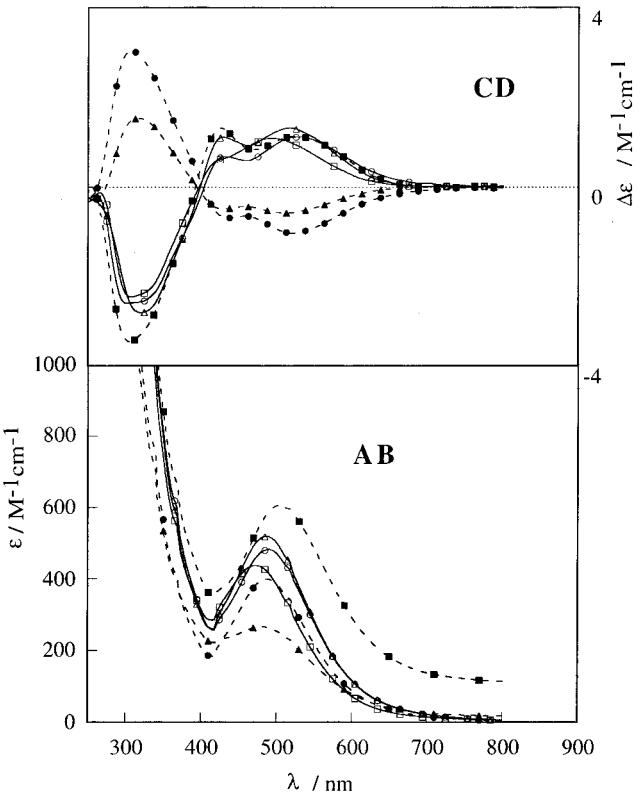

Figure 1. Electronic absorption (AB) and circular dichroism (CD) spectra of [{Mn((D-Man)$_3$-tren)}$_2$Mn(H$_2$O)]Cl$_3$ (**5a**) --●--, [{Mn((D-Man)$_3$-tren)}$_2$Mn(H$_2$O)]Br$_3$ (**5b**) --▲--, [{Mn((L-Rha)$_3$-tren)}$_2$Mn(H$_2$O)]Cl$_3$ (**6a**) −△−, [{Mn((L-Rha)$_3$-tren)}$_2$Mn(H$_2$O)]Br$_3$ (**6b**) −○−, [{Mn((L-Rha)$_3$-tren)}$_2$Mn(H$_2$O)](NO$_3$)$_3$ (**6c**) −□−, and [{Mn((L-Rha)$_3$-tren)}$_2$Mn(H$_2$O)](SO$_4$)$_{1.5}$ (**6d**) --■--, in methanol.

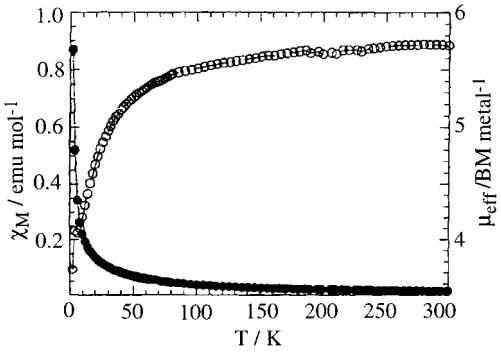

Figure 2. Plots of molar susceptibility, χ_M (●), and effective moment, μ_{eff} (○), for complex **6a** with the fits to eq 1 (solid line).

in intensity. Reflection data were corrected for Lorentz−polarization and absorption effects (ψ-scan method).

The structure of **3b**·3.5H$_2$O was solved by direct methods with SIR92.[12] The most non-hydrogen atoms were located initially, and subsequent Fourier syntheses gave the positions of other non-hydrogen atoms. The structure has a crystallographically imposed C_3 symmetry, and 1/3 atoms for the formula were determined independently. The coordinates of C−H and N−H hydrogen atoms were calculated at ideal positions with a distance of 0.95 Å and were not refined. The structure was refined with full-matrix least-squares techniques on F minimizing $\sum w(|F_o| - |F_c|)^2$. Final refinement with anisotropic thermal parameters for non-hydrogen atoms converged at $R = 0.059$ and $R_w = 0.061$, where $R = \sum||F_o| - |F_c||/\sum|F_o|$ and $R_w = [\sum w(|F_o| - |F_c|)^2/\sum w|F_o|^2]^{1/2}$ ($w = 1/\sigma^2(F_o)$). The structure of **4d**·4CH$_3$OH was solved by direct methods with SIR92. The most non-hydrogen atoms were located initially, and

(12) Burla, M. C.; Camalli, M.; Cascarano, G.; Giacovazzo, C.; Polidori, G.; Spagna, R.; Viterbo, D. *J. Appl. Crystallogr.* **1989**, *22*, 389.

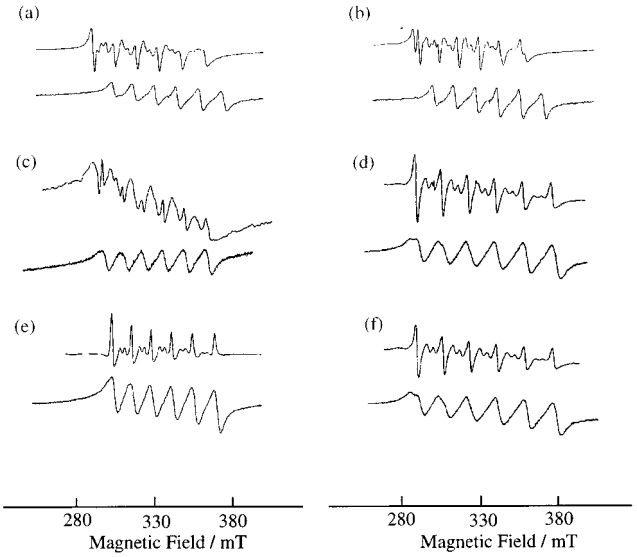

Figure 3. X-band EPR spectra of (a) **6a**, (b) **5b**, (c) **4d**, (d) **3b**, (e) **3a**, and (f) **3c**, at 77 K (upper) and 298 K (lower).

Table 3. Selected Bond Lengths and Angles of [Mn((D-Man)$_3$-tren)]Br$_2$ (**3b**)[a]

Bond Lengths (Å)			
Mn(1)−O(2)	2.291(5)	Mn(1)−N(1)	2.37(1)
Mn(1)−N(2)	2.292(6)	O(2)−C(2)	1.442(8)
O(3)−C(3)	1.439(9)	O(4)−C(4)	1.411(8)
O(5)−C(1)	1.412(8)	O(5)−C(5)	1.451(8)
O(6)−C(6)	1.431(8)	N(1)−C(11)	1.480(8)
N(2)−C(1)	1.492(9)	N(2)−C(12)	1.497(9)

Bond Angles (deg)			
O(2)−Mn(1)−O(2)*	80.0(2)	O(2)−Mn(1)−N(1)	132.1(1)
O(2)−Mn(1)−N(2)	74.9(2)	O(2)−Mn(1)−N(2)*	82.9(2)
O(2)−Mn(1)−N(2)**	151.7(2)	N(1)−Mn(1)−N(2)	75.7(1)
N(2)−Mn(1)−N(2)*	114.1(1)	Mn(1)−O(2)−C(2)	113.2(4)
Mn(1)−N(1)−C(11)	107.5(5)	Mn(1)−N(2)−C(1)	109.9(4)
Mn(1)−N(2)−C(12)	106.6(4)		

[a] Estimated standard deviations are given in parentheses.

subsequent cycles of full-matrix least-squares refinement and difference Fourier syntheses gave the positions of remaining non-hydrogen atoms. The coordinates of C−H and N−H hydrogen atoms were calculated at ideal positions with a distance of 0.95 Å and were not refined. Final full-matrix refinement with anisotropic thermal parameters for the Mn, S, O (except those of solvents), and N atoms and with isotropic ones for other non-hydrogen atoms converged at $R = 0.085$ and $R_w = 0.087$.

The structure of **5a**·6H$_2$O was solved by direct methods with SIR92, expanded by Fourier and difference Fourier syntheses, and refined with full-matrix least-squares techniques. The coordinates of C−H and N−H hydrogen atoms were calculated at ideal positions with a distance of 0.95 Å and were not refined. Final full-matrix refinement with anisotropic thermal parameters for the Mn, Cl, O (except those of solvents), and N atoms and with isotropic ones for other non-hydrogen atoms converged at $R = 0.083$ and $R_w = 0.091$. The structure of **5b**·8H$_2$O was solved and refined by a procedure similar to that for **5a**·6H$_2$O. Final refinement with anisotropic thermal parameters for the Mn, Br, O (except those of solvents), and N atoms and with isotropic ones for other non-hydrogen atoms converged at $R = 0.081$ and $R_w = 0.085$. The structure of **6c**·5H$_2$O was solved and refined by a procedure similar to that for **5a**·6H$_2$O. The structure has a crystallographically imposed C_2 symmetry, and half of the atoms for the formula were determined independently. Final refinement with anisotropic thermal parameters for the Mn, O (except those of solvents and nitrate anions), and N (except that of nitrate anions) atoms and with isotropic ones for other non-hydrogen atoms converged at $R = 0.073$ and $R_w = 0.073$. The structure of **6d**·8H$_2$O was solved and refined by a procedure similar to that for **5a**·6H$_2$O. The structure has a crystallographically imposed C_2 symmetry, and half of the atoms for the formula were determined

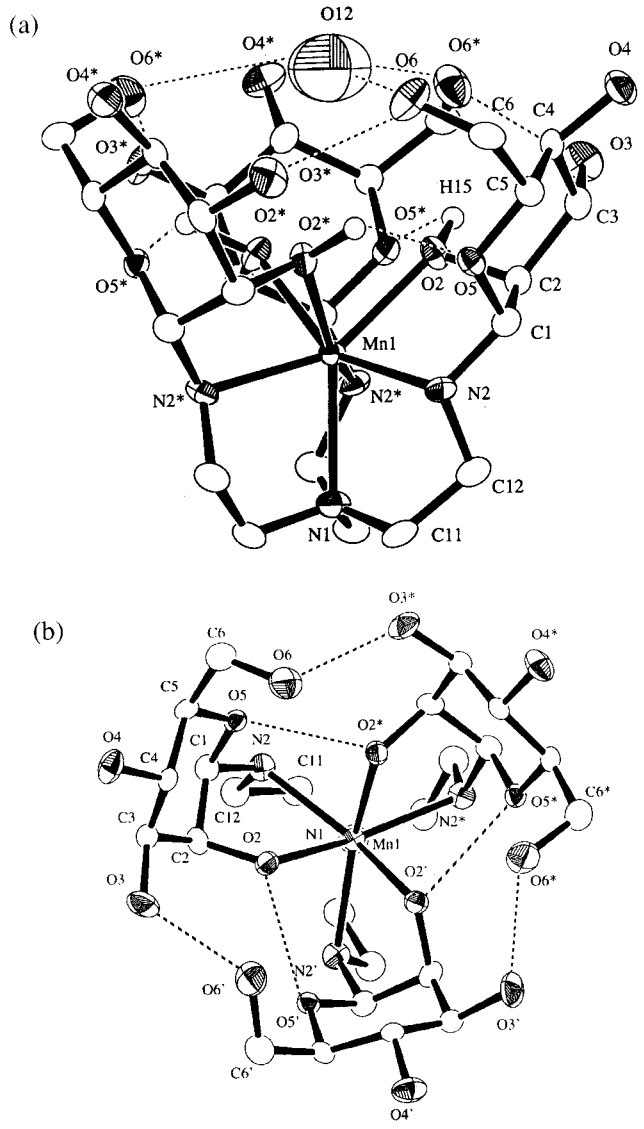

Figure 4. (a) ORTEP plot for the cation of $[Mn((D\text{-}Man)_3\text{-}tren)]Br_2$ (**3b**) with the trapped water molecule and (b) ORTEP plot of the cation viewed along the C_3 axis.

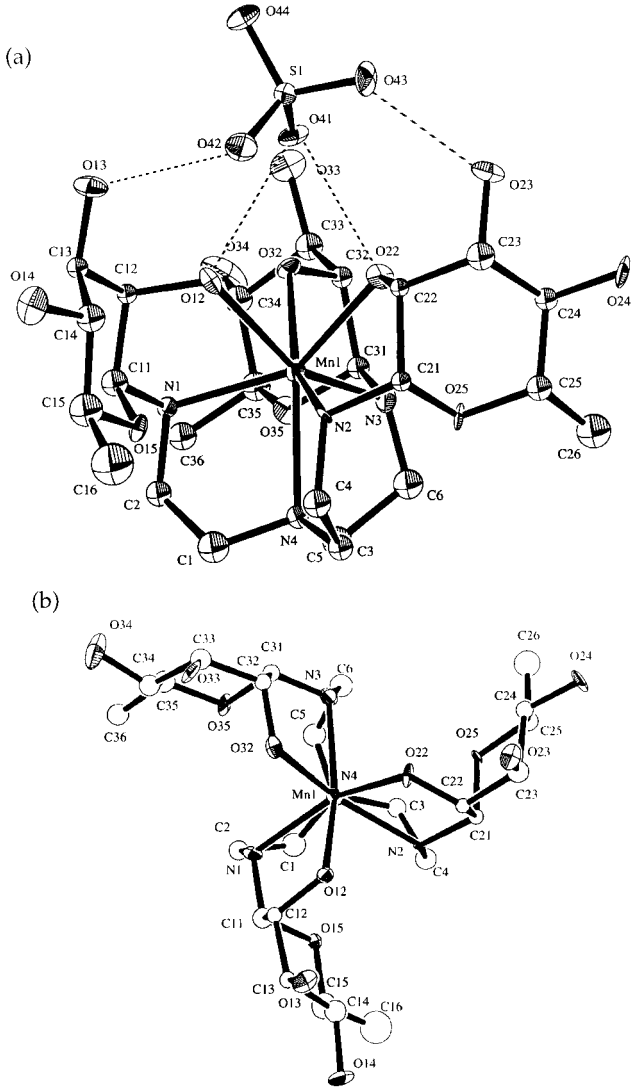

Figure 5. (a) ORTEP plot of $[Mn((L\text{-}Rha)_3\text{-}tren)]SO_4$ (**4d**) and (b) ORTEP plot of the cation viewed along the pseudo C_3 axis.

independently. Final refinement with anisotropic thermal parameters for all non-hydrogen atoms, those of solvents being refined isotropically, converged at $R = 0.061$ and $R_w = 0.073$.

The absolute configurations of all of the crystal structures were determined by using the known configurations of sugars as internal references. Atomic scattering factors and values of f' and f'' for Co, Br, S, Cl, O, N, and C were taken from the literature.[13,14] All calculations were carried out on Silicon Graphics Indigo, Indy, and O2 Stations with the teXsan program package.[15] The perspective views were drawn by using the program ORTEP.[16] Compilation of final atomic parameters for all non-hydrogen atoms is supplied as Supporting Information.

Results and Discussion

Preparation of Mn^{II} and $Mn^{II}Mn^{III}Mn^{II}$ Complexes with Heptadentate *N*-Glycoside Ligands. Synthetic routes and isolated Mn^{II} and $Mn^{II}Mn^{III}Mn^{II}$ complexes with heptadentate *N*-glycoside ligands, $(aldose)_3$-tren, in the present report are summarized in Scheme 1.

Reactions of Mn(II) salts, $MnX_2 \cdot nH_2O$, with tris(*N*-(D-mannosyl)-2-aminoethyl)amine ($(D\text{-}Man)_3$-tren), formed from tren and D-mannose in refluxing methanol, afforded colorless crystals formulated as $[Mn((D\text{-}Man)_3\text{-}tren)]X_2 \cdot nH_2O$ (**3a**$\cdot 5H_2O$, X = Cl; **3b**$\cdot 4H_2O$, X = Br; **3c**$\cdot 4H_2O$, X = NO_3; **3d**$\cdot 4H_2O$, X = $^1/_2SO_4$) in 20−82% yields (Scheme 1, method A). Similar reaction of $MnSO_4 \cdot 5H_2O$ with tris(*N*-(L-rhamnosyl)-2-aminoethyl)amine, $((L\text{-}Rha)_3$-tren), gave $[Mn((L\text{-}Rha)_3\text{-}tren)]SO_4 \cdot 4H_2O$ (**4d**$\cdot 4H_2O$) in 42% yield (Scheme 1). The elemental analysis showed a mononuclear manganese ion to be ligated by the potentially heptadentate *N*-glycoside ligand, $aldose_3$-tren, and the effective magnetic moments (5.62−5.89 μ_B) indicated the high-spin Mn(II) state. The X-ray crystallographic analyses of **3b** and **4d** indicated that complexes **3a**−**d** and **4d** are seven-coordinate mononuclear Mn(II) complexes ligated by the $(aldose)_3$-tren *N*-glycoside ligand through $[N_4O_3]$ donor atoms (vide infra).

When complexes **3a**, **3b**, and **4d** were treated with 0.5 equiv of the corresponding Mn(II) salt, $MnX_2 \cdot nH_2O$, in the presence of triethylamine, reddish orange crystals of $[\{Mn(aldose)_3\text{-}tren\}_2Mn(H_2O)]X_3 \cdot nH_2O$ (**5a**$\cdot 6.5H_2O$, X = Cl, aldose = D-Man; **5b**$\cdot 4H_2O$, X = Br, aldose = D-Man; **6d**$\cdot 7H_2O$, X = $^1/_2SO_4$, aldose = L-Rha) were obtained in 20%, 26%, and 19% yields, respectively (Scheme 1, method B). Complexes **5a**, **5b**,

(13) Cromer, D. T. *Acta Crystallogr.* **1965**, *18*, 17.
(14) Cromer, D. T.; Waber, J. T. *International Tables for X-ray Crystallography*; Kynoch Press: Birmingham, England, 1974.
(15) *TEXSAN Structure Analysis Package*; Molecular Structure Corporation: The Woodlands, TX, 1985.
(16) Johnson, C. K. Oak Ridge National Laboratory: Oak Ridge, TN, 1976.

Table 4. Selected Bond Lengths and Angles of $[Mn((L\text{-}Rha)_3\text{-tren})]SO_4$ (**4d**)[a]

Bond Lengths (Å)			
Mn(1)−O(12)	2.34(1)	Mn(1)−O(22)	2.314(9)
Mn(1)−O(32)	2.368(9)	Mn(1)−N(1)	2.27(1)
Mn(1)−N(2)	2.28(1)	Mn(1)−N(3)	2.27(1)
Mn(1)−N(4)	2.44(1)		
S(1)−O(41)	1.51(1)	S(1)−O(42)	1.46(1)
S(1)−O(43)	1.49(1)	S(1)−O(44)	1.47(1)

Bond Angles (deg)			
O(12)−Mn(1)−O(22)	75.4(4)	O(12)−Mn(1)−O(32)	80.6(3)
O(12)−Mn(1)−N(1)	72.7(4)	O(12)−Mn(1)−N(2)	84.9(4)
O(12)−Mn(1)−N(3)	151.6(4)	O(12)−Mn(1)−N(4)	132.6(4)
O(22)−Mn(1)−O(32)	80.4(4)	O(22)−Mn(1)−N(1)	147.7(4)
O(22)−Mn(1)−N(2)	73.2(4)	O(22)−Mn(1)−N(3)	91.6(4)
O(22)−Mn(1)−N(4)	133.4(4)	O(32)−Mn(1)−N(1)	89.3(4)
O(32)−Mn(1)−N(2)	152.4(4)	O(32)−Mn(1)−N(3)	72.3(4)
O(32)−Mn(1)−N(4)	132.5(4)	N(1)−Mn(1)−N(2)	108.6(4)
N(1)−Mn(1)−N(3)	114.4(4)	N(1)−Mn(1)−N(4)	74.8(4)
N(2)−Mn(1)−N(3)	115.9(4)	N(2)−Mn(1)−N(4)	73.8(4)
N(3)−Mn(1)−N(4)	74.4(4)		
O(41)−S(1)−O(42)	108.5(6)	O(41)−S(1)−O(43)	109.2(6)
O(41)−S(1)−O(44)	107.2(6)	O(42)−S(1)−O(43)	109.2(7)
O(42)−S(1)−O(44)	112.1(7)	O(43)−S(1)−O(44)	110.5(7)

[a] Estimated standard deviations are given in parentheses.

and **6d** were shown by X-ray crystallography to be novel Mn^{II}-$Mn^{III}Mn^{II}$ mixed valence trimanganese complexes with the $(aldose)_3$-tren ligand (vide infra). The reactions were monitored by UV−vis and CD spectra, indicating that yields of the trimanganese complexes in situ were moderate despite relatively low isolated yields as crystalline compounds. In the absence of Et_3N, the color of the reaction solution did not change and no crystalline compounds were isolated from the solution. Treatment of $MnX_2 \cdot nH_2O$ with Et_3N, without the presence of the Mn(II)-sugar complexes, led exclusively to deposition of MnO_2 from methanolic solution. These results demonstrated that the added Mn(II) ion was encapsulated between two mononuclear Mn(II) complexes (**3**, **4**) and the trapped central Mn(II) ion was further oxidized to Mn(III) under aerobic conditions by the action of Et_3N to form the stable $Mn^{II}Mn^{III}Mn^{II}$ complexes (**5**, **6**). When the reactions were carried out under nitrogen, formation of the $Mn^{II}Mn^{III}Mn^{II}$ complexes was dramatically suppressed, suggesting that dioxygen was an oxidant. Unfortunately, we have not been successful in isolating the postulated Mn^{II}_3 species, which might be more structurally relevant to xylose isomerases, despite some attempts to do so. The terminal Mn(II) centers were not oxidized during the reaction because they are sterically protected by the heptadentate cage-type *N*-glycoside ligand. An estimated mechanism is illustrated in Scheme 2. Similar treatment of **3c** and **3d** did not work for preparation of trimanganese complexes due presumably to their poor solubility in methanol.

Reactions of $MnX_2 \cdot nH_2O$ with $(L\text{-}Rha)_3$-tren yielded a series of trimanganese complexes, $[\{Mn((L\text{-}Rha)_3\text{-tren})\}_2Mn(H_2O)]X_3 \cdot nH_2O$ (**6a**·$11H_2O$, X = Cl; **6b**·$10H_2O$, X = Br; **6c**·$8H_2O$, X = NO_3), in 31−43% yields (Scheme 1, method A). In the case using L-Rha as a sugar source, mononuclear Mn(II) complexes with a $(L\text{-}Rha)_3$-tren ligand, postulated intermediate species to the trimanganese complexes, were not isolated, suggesting that Mn(II) complexes with $(L\text{-}Rha)_3$-tren are more unstable and/or reactive toward metal assembling than the corresponding isolated complexes with $(D\text{-}Man)_3$-tren (**3a**−**c**).

Spectral and Magnetic Properties. The trimanganese−sugar complexes (**5a**,**b** and **6a**,**d**) were assumed to have almost identical structures on the basis of IR spectra and electronic absorption and circular dichroism spectra and magnetic susceptibilities. The electronic absorption spectra of **5** and **6** in methanol showed a characteristic band around 470−505 nm ascribable to a Mn(III)−ligand charge transfer band, and appreciable Cotton effects were observed in the same region of the CD spectra, indicating that the Mn(III) center was ligated by chiral sugar moieties (Figure 1). The CD spectral patterns of complexes **5**, involving D-mannose residues, are almost mirror images of those of complexes **6** with L-rhamnose (6-deoxy-L-mannose) moieties, with respect to the $\Delta\epsilon = 0$ line.

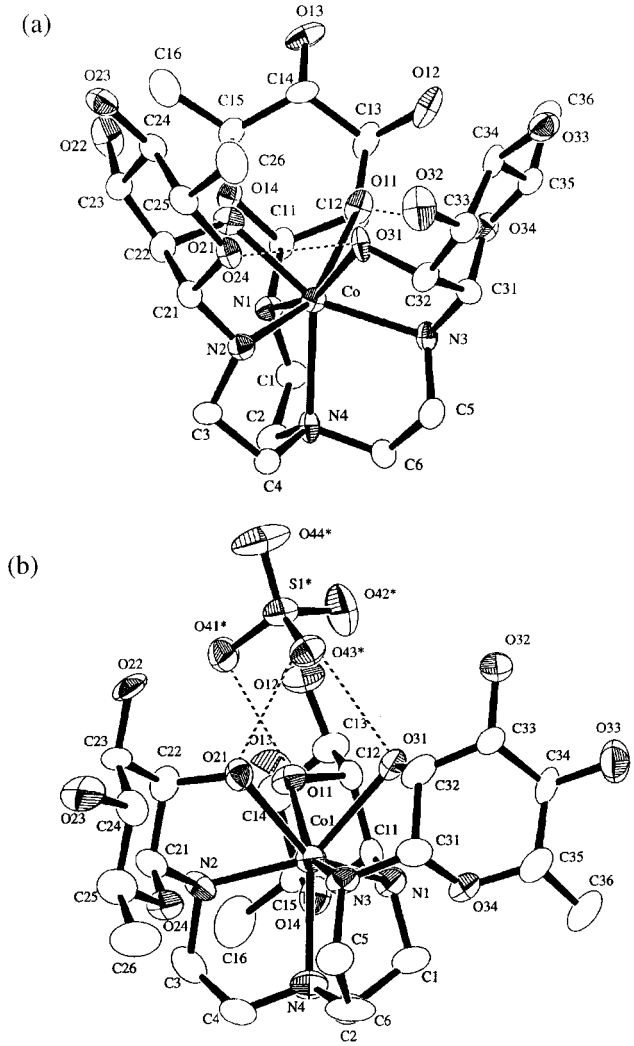

Figure 6. ORTEP diagrams of (a) $[Co((L\text{-}Rha)_3\text{-tren})]Br_2$ (**2b**) and (b) $[Co((L\text{-}Rha)_3\text{-tren})](SO_4)$ (**2d**) (ref 9).

Values of μ_{eff} at room temperature range from 8.46 to 9.28 μ_B, μ_{eff} per metal being 4.88−5.36 μ_B, these values being smaller than those of the Mn(II)−sugar complexes **3** and **4** (5.62−5.89 μ_B). Variable-temperature magnetic susceptibility data (4−300 K) were measured for complexes **6a**−**c**. The Hamiltonian, $H = -2[J_{12}S_1 \cdot S_2 + J_{23}S_2 \cdot S_3 + J_{13}S_1 \cdot S_3] + \mu_B[g_1S_1 + g_2S_2 + g_3S_3] \cdot B$, was employed in the analysis of the magnetic data, where $S_1 = S_3 = {}^5/_2$, $S_2 = 2$, $J_{12} = J_{23} = J$, $J_{13} = J'$, and $g_1 = g_2 = g_3 = g$. The data were fit as the molar magnetic susceptibility to eq 1, which is derived from the field-independent Van Vleck equation. The exchange energies were

$$\chi_M = (Ng^2\mu_B{}^2/3kT)\frac{[\Sigma_i S_i(S_i+1)(2S_i+1)\exp(-E_i/kT)]}{[\Sigma_i(2S_i+1)\exp(-E_i/kT)]} \quad (1)$$

Chart 1

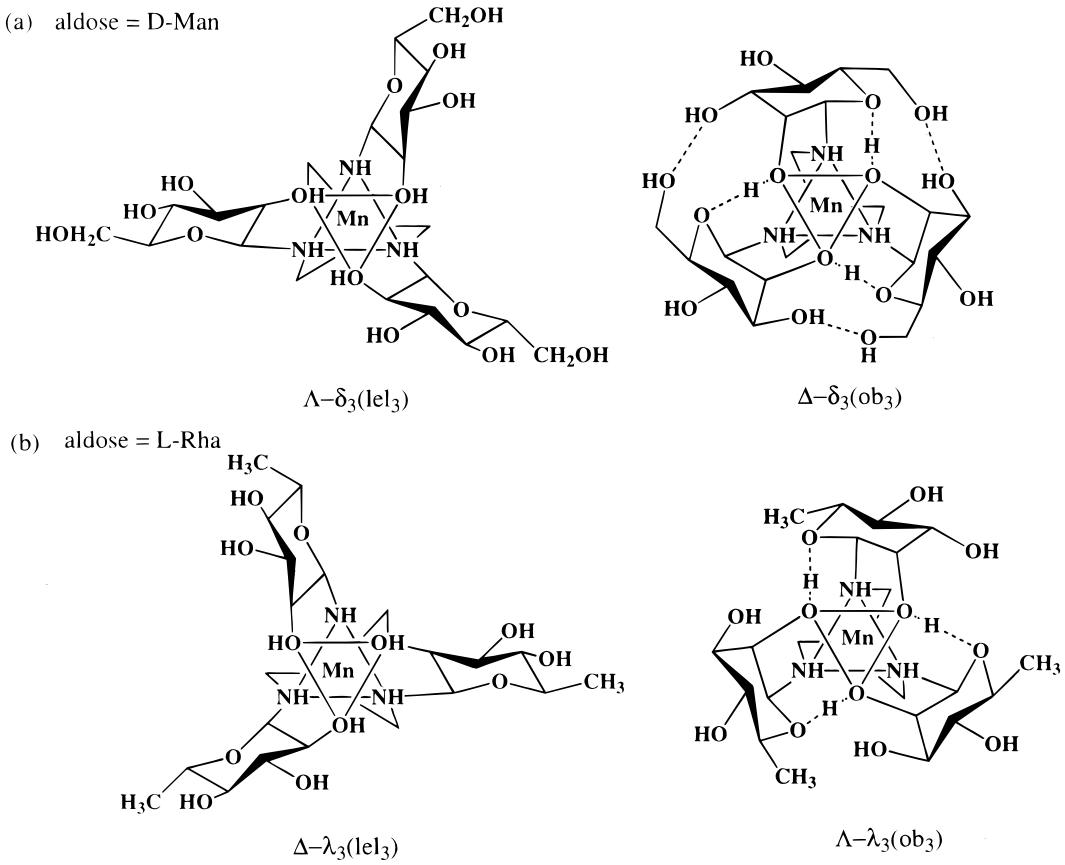

calculated by Kambe's method.[17] The best fits were obtained when J, J', and g were allowed to vary simultaneously, refining to values of $J = -1.3$ cm^{-1} (**6a**), -1.2 cm^{-1} (**6b**), -1.4 cm^{-1} (**6c**), $J' = 0.3$ cm^{-1} (**6a**), 0.3 cm^{-1} (**6b**), 0.2 cm^{-1} (**6c**), and $g = 2.07$ (**6a**), 1.95 (**6b**), 1.97 (**6c**) (Figure 2). The values of J (-1.2 to -1.4 cm^{-1}) indicate that only weak antiferromagnetic coupling is mediated by the monodentate μ-alkoxo sugar bridging, and those of J' are negligible ($\approx$0) on the basis of relatively large zero-field splitting of Mn(II) ions.[18] The observed Mn(II)···Mn(III) antiferromagnetic interaction (Mn···Mn = 3.845 Å) is weaker than those found in the $Mn^{III}Mn^{II}$-Mn^{III} complexes ($J = -3$ to -7 cm^{-1} for Mn···Mn = 3.419−3.551 Å).[19−24]

The EPR spectra of **5b** and **6a** in methanol at 298 K were dominated by the simple six-line signal around $g_0 = 2.01$ which is characteristic of a high-spin isotropic Mn(II) ion and might arise either from a partial detection of only the terminal Mn(II) units or a partially dissociated Mn^{II} species (Figure 3a,b). In the low-temperature (77 K) spectra, the six-line spectral pattern was retained with some complicated splittings. This spectral feature was very similar to those observed for the mononuclear manganese(II) complexes **3a**−**c** and **4d** (Figure 3c−f).

Structures of Mononuclear Mn(II)−Sugar Complexes. The structures of **3b** and **4d** were determined by X-ray crystallography. ORTEP plots of **3b** and **4d** are illustrated in Figures 4 and 5, and selected bond distances and angles are listed in Tables 3 and 4.

The complex cation in **3b** possesses a crystallographically imposed C_3 symmetry with the axis passing through the Mn(1) and N(1) atoms and comprises a mononuclear Mn(II) ion ligated by a heptadentate *N*-glycoside ligand, (D-Man)$_3$-tren (Figure 4), which is similar to the structure of [Co((L-Rha)$_3$-tren)]Br$_2$ (**2b**)[9c] except for the C-6 hydroxyl groups (Figure 6a). The ligand coordinates to the metal through four nitrogen atoms and three C-2 hydroxyl groups of sugar moieties to complete a considerably distorted mono-face-capped octahedral geometry. The tertiary amino nitrogen of the tren part binds to the facial site with the Mn−N distance being 2.375(9) Å. The bite angles of O(2)−Mn(1)−N(2) and N(1)−Mn(1)−N(2) are 74.7(2)° and 75.9(1)°, respectively. The three sugar units adopt a $^4C_1$ chair pyranosyl conformation and are anchored on the amino groups of tren with a β-N-glycosidic bond. The five-membered chelate rings of the sugar moieties take a δ-gauche conformation and are arranged in *ob* form with respect to the C_3 axis, resulting in a $\Delta(ob_3)$ C_3-helical configuration around the metal. The relatively crowded $\Delta(ob_3)$ structure is stabilized by inter-sugar hydrogen bonding networks, O(2)···O(5)* = 2.746(6) Å, O(3)···O(6)* = 2.753(6) Å, resulting in a cage-type closed sugar domain. The sugar−sugar interactions in **3b** should be stronger

(17) (a) Kambe, K. *J. Phys. Soc. Jpn.* **1950**, *5*, 48. (b) Allen, D. W.; Nowell, I. W.; Taylor, B. F. *J. Chem. Soc., Dalton Trans.* **1985**, 2505.
(18) Baldwin, M. J.; Kampf, J. W.; Kirk, M. L.; Pecoraro, V. L. *Inorg. Chem.* **1995**, *34*, 5252.
(19) Tangouls, V.; Malamatari, D. A.; Soulti, K.; Stergiou, V.; Raptopoulou, C. P.; Terzis, A.; Kabanos, T. A.; Kessissoglou, D. P. *Inorg. Chem.* **1996**, *35*, 4974.
(20) Li, X.; Kessissoglou, D. P.; Kirk, M. L.; Bender, C. J.; Pecoraro, V. L. *Inorg. Chem.* **1988**, *27*, 1.
(21) Kessissoglou, D. P.; Kirk, M. L.; Bender, C. A.; Lah, M. S.; Pecoraro, V. L. *J. Chem. Soc., Chem. Commun.* **1989**, 84.
(22) Kessissoglou, D. P.; Kirk, M. L.; Lah, M. S.; Li, X.; Raptopoulou, C.; Hatfield, W. E.; Pecoraro, V. L. *Inorg. Chem.* **1992**, *31*, 5424.
(23) Malamatari, D. A.; Hitou, P.; Hatzidimitriou, A. G.; Inscore, F. E.; Gourdon, A.; Kirk, M. L.; Kessissoglou, D. P. *Inorg. Chem.* **1995**, *34*, 2493.
(24) Kitajima, N.; Osawa, M.; Imai, S.; Fujisawa, K.; Moro-oka, Y.; Heerwegh, K.; Reed, C. A.; Boyd, P. D. W. *Inorg. Chem.* **1994**, *33*, 4613.

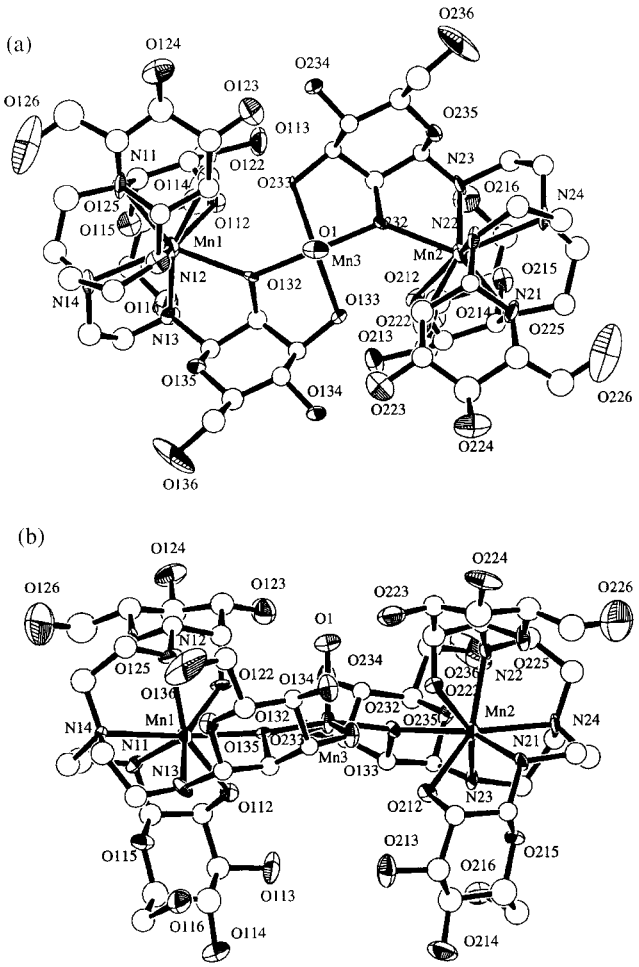

Figure 7. ORTEP plots for the trimanganese cation of $[\{Mn((D\text{-}Man)_3\text{-}tren)\}_2Mn(H_2O)]Br_3$ (**5b**) (a) viewed along the pseudo C_2 axis and (b) viewed perpendicular to the axis.

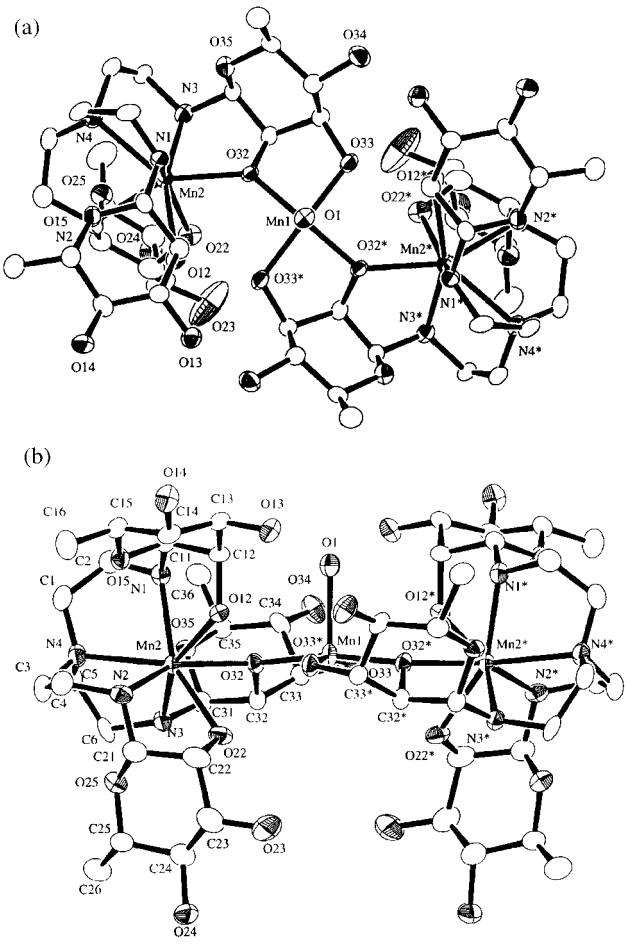

Figure 8. ORTEP plots for the trimanganese cation of $[\{Mn((L\text{-}Rha)_3\text{-}tren)\}_2Mn(H_2O)](SO_4)_{1.5}$ (**6d**) (a) viewed along the C_2 axis and (b) viewed perpendicular to the C_2 axis.

than those found in **2b** owing to the presence of C-6 hydroxyl groups. Further, a water molecule is loosely trapped in the narrow cavity composed of the three D-mannose residues (O(6)···O(12) = 3.273(6) Å), which might further stabilize the closed sugar domain.

The complex cation of **4d** has a pseudo C_3 symmetry, consisting of a Mn(II) ion with a cage-type ligand (Figure 5), (L-Rha)$_3$-tren, just like [Co((L-Rha)$_3$-tren)]SO$_4$ (**2d**) (Figure 6b).[9c] The *N*-glycoside acts as a heptadentate ligand with the tertiary amino nitrogen capping a facial site with a Mn−N distance of 2.44(1) Å. The β-L-rhamnopyranosyl units take $^4C_1$ chair conformations and are attached to the metal through the N-glycosidic nitrogen atom and C-2 hydroxyl oxygen atom. The C_3 helical configuration is $\Delta(lel_3)$ with three λ-gauche sugar chelations. The other facial site, composed of three C-2 hydroxyl groups of sugar moieties, is capped by a sulfate anion supported by hydrogen bonding (O(12)···O(41) = 2.78(1) Å, O(22)···O(41) = 2.78(1) Å, O(13)···O(42) = 2.77(1) Å, O(23)···O(43) = 2.64(1) Å). The sulfate anion is considerably distorted from a C_3 symmetrical structure in comparison with that found in **2d**. The Mn(1)···S(1) interatomic distance is 5.237(5) Å, which is significantly longer than is found in **2d** (Co···S = 4.697(6) Å), and indicates a weaker ion-pair interaction than in **2d**.

Comparison of the structural parameters of **3b** and **4d** with those of the corresponding cobalt(II) complexes **2b** and **2d** is useful to understand the differences between the properties of the Mn(II) and Co(II) complexes. All coordination bond lengths of **3b** and **4d** are longer than those of **2b** and **2d**, respectively, which suggested that the Mn(II)−sugar complexes are more flexible than the Co(II)−sugar complexes. In fact, the Co(II)−sugar complexes **1** and **2** did not have metal-trapping ability by the sugar domain as observed in the formation of the trimanganese complexes which required a chiral inversion around the Mn(II) center, from an ob_3 configuration to an lel_3 one (see structures of the trimanganese complexes).

The two types of C_3 helical configurations, Λ-$\delta_3(ob_3)$ and Δ-$\delta_3(lel_3)$, should be considered, in general, for the D-mannose-containing complex, $[Mn((D\text{-}Man)_3\text{-}tren)]^{2+}$, as depicted in Chart 1a. The structures of $[Mn((L\text{-}Rha)_3\text{-}tren)]^{2+}$ are essentially enantiomeric to the corresponding D-mannose complexes because L-Rha is an enantiomer to D-Man except for the C-6 substituent group (Chart 1b). The present structural analyses clearly revealed that the configurational switch of the metal center proceeds depending on the counteranions; the ob_3 form, found with bromide anions, bears a small and deep cavity on the sugar-facial site which is stabilized by hydrogen bonds between the sugar ligands, and, on the other hand, the lel_3 form has a wide and shallow cavity which is capped by a sulfate anion.

Structures of $Mn^{II}Mn^{III}Mn^{II}$ Trinuclear Complexes with Sugar Ligands. The structures of **5a**, **5b**, **6c**, and **6d** were determined by X-ray crystallographic analyses. ORTEP drawings of the complex cations are depicted in Figures 7 (**5b**) and 8 (**6d**), and selected bond distances and angles are listed in Tables 5 and 6. Perspective drawings of **5a** and **6c** are supplied as Supporting Information.

Table 5. Selected Bond Lengths and Angles of $[\{Mn((D\text{-}Man)_3\text{-}tren)\}_2Mn(H_2O)]X_3$ (X = Cl (**5a**), Br (**5b**))[a]

	5a (X = Cl)	**5b** (X = Br)		**5a** (X = Cl)	**5b** (X = Br)
			Bond Lengths (Å)		
Mn(1)−O(112)	2.35(2)	2.32(1)	Mn(2)−N(21)	2.27(2)	2.29(2)
Mn(1)−O(122)	2.46(2)	2.48(1)	Mn(2)−N(22)	2.32(2)	2.27(2)
Mn(1)−O(132)	2.31(2)	2.28(1)	Mn(2)−N(23)	2.28(2)	2.27(2)
Mn(1)−N(11)	2.26(2)	2.29(2)	Mn(2)−N(24)	2.42(2)	2.44(2)
Mn(1)−N(12)	2.26(2)	2.27(2)	Mn(3)−O(1)	2.19(1)	2.17(1)
Mn(1)−N(13)	2.28(2)	2.28(2)	Mn(3)−O(132)	1.88(2)	1.91(1)
Mn(1)−N(14)	2.46(2)	2.44(2)	Mn(3)−O(133)	1.96(2)	1.93(1)
Mn(2)−O(212)	2.32(2)	2.33(1)	Mn(3)−O(232)	1.90(2)	1.93(1)
Mn(2)−O(222)	2.44(2)	2.50(2)	Mn(3)−O(233)	1.93(2)	1.93(1)
Mn(2)−O(232)	2.30(2)	2.29(1)			
			Bond Angles (deg)		
O(112)−Mn(1)−O(122)	77.3(5)	76.9(5)	O(212)−Mn(2)−N(24)	133.5(6)	135.1(5)
O(112)−Mn(1)−O(132)	74.4(5)	73.9(4)	O(222)−Mn(2)−O(232)	82.8(5)	83.2(5)
O(112)−Mn(1)−N(11)	71.7(6)	72.7(5)	O(222)−Mn(2)−N(21)	82.0(6)	82.6(5)
O(112)−Mn(1)−N(12)	147.6(6)	147.3(6)	O(222)−Mn(2)−N(22)	72.8(6)	71.4(6)
O(112)−Mn(1)−N(13)	90.0(6)	91.4(6)	O(222)−Mn(2)−N(23)	157.6(6)	156.4(5)
O(112)−Mn(1)−N(14)	133.1(6)	135.5(5)	O(222)−Mn(2)−N(24)	128.2(5)	128.3(5)
O(122)−Mn(1)−O(132)	82.4(5)	82.8(4)	O(232)−Mn(2)−N(21)	145.8(6)	145.7(5)
O(122)−Mn(1)−N(11)	82.5(6)	83.0(5)	O(232)−Mn(2)−N(22)	92.2(6)	93.9(5)
O(122)−Mn(1)−N(12)	71.8(6)	71.6(6)	O(232)−Mn(2)−N(23)	75.8(6)	74.1(5)
O(122)−Mn(1)−N(13)	157.4(6)	157.8(6)	O(232)−Mn(2)−N(24)	137.4(6)	136.1(5)
O(122)−Mn(1)−N(14)	129.5(6)	128.4(5)	N(21)−Mn(2)−N(22)	112.1(6)	110.8(6)
O(132)−Mn(1)−N(11)	145.1(6)	145.9(5)	N(21)−Mn(2)−N(23)	112.4(7)	112.9(6)
O(132)−Mn(1)−N(12)	91.9(6)	93.4(6)	N(21)−Mn(2)−N(24)	74.6(7)	75.7(6)
O(132)−Mn(1)−N(13)	76.2(6)	75.8(5)	N(22)−Mn(2)−N(23)	114.1(7)	115.8(6)
O(132)−Mn(1)−N(14)	137.3(6)	136.5(5)	N(22)−Mn(2)−N(24)	74.4(6)	73.6(6)
N(11)−Mn(1)−N(12)	112.8(6)	111.1(6)	N(23)−Mn(2)−N(24)	73.6(6)	74.3(6)
N(11)−Mn(1)−N(13)	111.4(7)	111.8(6)	O(1)−Mn(3)−O(132)	97.3(6)O	97.6(5)
N(11)−Mn(1)−N(14)	74.9(7)	75.1(6)	O(1)−Mn(3)−O(133)	98.3(6)	99.3(6)
N(12)−Mn(1)−N(13)	115.5(7)	115.0(6)	O(1)−Mn(3)−O(232)	97.0(6)	96.9(6)
N(12)−Mn(1)−N(14)	76.3(7)	73.8(6)	O(1)−Mn(3)−O(233)	100.0(6)	99.4(6)
N(13)−Mn(1)−N(14)	72.7(7)	72.9(6)	O(132)−Mn(3)−O(133)	86.7(6)	87.0(5)
O(212)−Mn(2)−O(222)	77.4(5)	77.6(5)	O(132)−Mn(3)−O(232)	165.6(6)	165.5(5)
O(212)−Mn(2)−O(232)	75.0(5)	74.2(4)	O(132)−Mn(3)−O(233)	91.4(6)	91.1(5)
O(212)−Mn(2)−N(21)	71.8(6)	72.3(5)	O(133)−Mn(3)−O(232)	90.9(6)	91.2(5)
O(212)−Mn(2)−N(22)	148.8(6)	147.9(6)	O(133)−Mn(3)−O(233)	161.6(6)	161.3(6)
O(212)−Mn(2)−N(23)	90.6(6)	90.0(5)	O(232)−Mn(3)−O(233)	86.3(6)	86.0(5)

[a] Estimated standard deviations are given in parentheses.

Table 6. Selected Bond Lengths and Angles of $[\{Mn((L\text{-}Rha)_3\text{-}tren)\}_2Mn(H_2O)]X_3$ (X = NO_3 (**6c**), $^1/_2SO_4$ (**6d**))[a]

	6c (X = NO_3)	**6d** (X = $^1/_2SO_4$)		**6c** (X = NO_3)	**6d** (X = $^1/_2SO_4$)
			Bond Lengths		
Mn(1)−O(1)	2.16(1)	2.203(8)	Mn(2)−O(32)	2.251(8)	2.248(5)
Mn(1)−O(32)	1.890(7)	1.909(5)	Mn(2)−N(1)	2.25(1)	2.251(7)
Mn(1)−O(33)	1.920(8)	1.920(6)	Mn(2)−N(2)	2.24(1)	2.281(7)
Mn(2)−O(12)	2.299(9)	2.461(6)	Mn(2)−N(3)	2.23(1)	2.289(7)
Mn(2)−O(22)	2.574(8)	2.330(6)	Mn(2)−N(4)	2.43(1)	2.463(6)
			Bond Angles (deg)		
O(1)−Mn(1)−O(32)	96.8(3)	95.8(2)	O(22)−Mn(2)−N(2)	70.7(3)	72.6(2)
O(1)−Mn(1)−O(33)	99.7(3)	97.1(2)	O(22)−Mn(2)−N(3)	158.2(3)	86.7(2)
O(32)−Mn(1)−O(32)*	166.4(5)	168.5(3)	O(22)−Mn(2)−N(4)	127.2(3)	132.5(2)
O(32)−Mn(1)−O(33)	86.4(3)	86.1(2)	O(32)−Mn(2)−N(1)	147.4(3)	92.4(2)
O(32)−Mn(1)−O(33)*	91.3(3)	92.4(2)	O(32)−Mn(2)−N(2)	91.8(3)	147.2(2)
O(33)−Mn(1)−(33)*	160.7(5)	165.7(4)	O(32)−Mn(2)−N(3)	74.9(3)	75.2(2)
O(12)−Mn(2)−O(22)	77.6(3)	80.5(2)	O(32)−Mn(2)−N(4)	135.5(3)	135.3(2)
O(12)−Mn(2)−O(32)	76.1(3)	85.3(2)	N(1)−Mn(2)−N(2)	108.2(4)	111.2(2)
O(12)−Mn(2)−N(1)	73.1(3)	71.4(2)	N(1)−Mn(2)−N(3)	114.7(4)	116.8(2)
O(12)−Mn(2)−N(2)	146.9(3)	81.4(2)	N(1)−Mn(2)−N(4)	75.8(3)	74.5(2)
O(12)−Mn(2)−N(3)	88.8(3)	158.8(2)	N(2)−Mn(2)−N(3)	118.0(4)	110.9(2)
O(12)−Mn(2)−N(4)	134.0(3)	127.4(2)	N(2)−Mn(2)−N(4)	75.3(4)	75.0(2)
O(22)−Mn(2)−O(32)	85.2(3)	75.7(2)	N(3)−Mn(2)−N(4)	74.4(3)	73.6(2)
O(22)−Mn(2)−N(1)	77.9(3)	150.4(2)			

[a] Estimated standard deviations are given in parentheses.

The crystal structures of $[\{Mn((D\text{-}Man)_3\text{-}tren)\}_2Mn(H_2O)]X_3$ (**5a**, X = Cl; **5b**, X = Br) are isomorphous, and the asymmetric unit contains one complex cation and three halide anions. The halide anions are away from the metal centers and exert no influence on the complex structures. The complex cations have a pseudo C_2 symmetry and comprise a linearly ordered trimanganese core bridged by two carbohydrate residues (Figure 7). The average Mn···Mn separations are 3.911(7) Å (**5a**) and 3.916(6) Å (**5b**), and the Mn···Mn···Mn angles are 171.0(1)° (**5a**) and 170.7(1)° (**5b**). The terminal Mn atoms are seven-coordinate with a distorted mono-face-capped octahedral geometry ligated by the $(D\text{-}Man)_3$-tren ligand through three oxygen atoms of C-2 hydroxyl groups, three N-glycosidic nitrogen atoms, and a tertiary amino nitrogen atom. The geometrical and

Table 7. Structural Parameters of $Mn^{II}Mn^{III}Mn^{II}$ Complexes $[\{Mn(aldose)_3\text{-tren}\}_2Mn(H_2O)]X_3$[a]

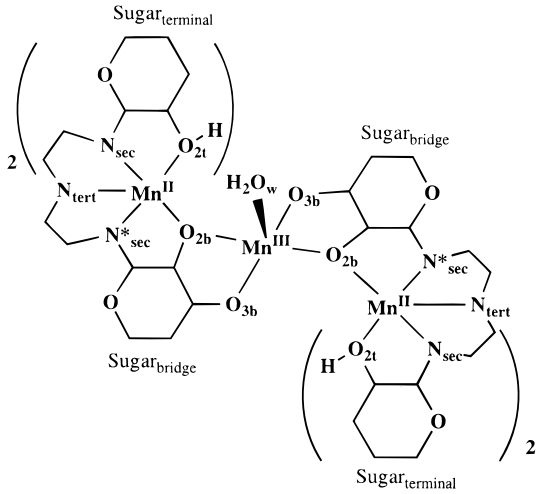

parameters	5a	5b	6c	6d	4d[b]	3b[b]
aldose	D-Man	D-Man	L-Rha	L-Rha	L-Rha	D-Man
counteranion	Cl^-	Br^-	NO_3^-	SO_4^{2-}	SO_4^{2-}	Br^-
$Mn^{II}\cdots Mn^{III}$, Å	3.911	3.916	3.845(2)	3.855(1)		
$Mn^{II}\cdots Mn^{III}\cdots Mn^{II}$, deg	171.0(1)	170.7(1)	173.9(1)	173.81(7)		
$Mn^{III}-O_w$, Å	2.19(1)	2.17(1)	2.16(1)	2.203(8)		
$Mn^{III}-O_{2b}$, Å	1.89	1.92	1.890(7)	1.909(4)		
$Mn^{III}-O_{3b}$, Å	1.95	1.93	1.920(8)	1.920(6)		
$O_{2b}-Mn^{III}-O_{3b}$, deg	86.5	86.5	86.4(3)	86.1(2)		
$Mn^{III}-O_{2b}-Mn^{II}$, deg	137.7	137.1	136.2(4)	135.9(3)		
$Mn^{II}-O_{2b}$, Å	2.31	2.29	2.251(8)	2.248(5)		
$Mn^{II}-O_{2t}$, Å	2.34	2.33	2.299(9)	2.330(6)	2.34(1)	2.287(5)
	2.45	2.49	2.574(8)	2.461(6)	2.314(9)	
					2.368(9)	
$Mn^{II}-N^*_{sec}$, Å	2.28	2.28	2.23(1)	2.289(7)		
$Mn^{II}-N_{sec}$, Å	2.27	2.29	2.254(10)	2.251(7)	2.27(1)	2.285(6)
	2.29	2.27	2.24(1)	2.281(7)	2.28(1)	
					2.27(1)	
$Mn^{II}-N_{tert}$, Å	2.44	2.44	2.428(10)	2.463(6)	2.44(1)	2.375(9)
$O_{2b}-Mn^{II}-N^*_{sec}$, deg	76.0	75.0	74.9(3)	75.2(2)		
$O_{2t}-Mn^{II}-N_{sec}$, deg	72.0	72.0	71.9	72.0	72.7	74.7(2)
$N^*_{sec}-Mn^{II}-N_{tert}$, deg	73.2	73.6	74.4(3)	73.6(2)		
$N_{sec}-Mn^{II}-N_{tert}$, deg	75.1	74.6	75.6	74.8	74.3	75.9(1)

[a] Average values are given without estimated standard deviations in parentheses. [b] Mononuclear Mn(II) complexes; $[Mn((D\text{-Man})_3\text{-tren})]Br_2$ (**3b**) and $[Mn((L\text{-Rha})_3\text{-tren})]SO_4$ (**4d**).

configurational aspects for the terminal Mn centers are essentially identical to those observed in $[Mn((L\text{-Rha})_3\text{-tren})]SO_4$ (**4d**); this strongly demonstrated the Mn(II) oxidation state for the terminal Mn ions in **5** (Table 7). The C_3 helical configurations and the sugar chelate conformations are denoted as Λ-*lel*(δ_3), which is an inverted structure of Δ-ob$_3$(δ_3) found in $[Mn((D\text{-Man})_3\text{-tren})]Br_2$ (**3b**). Namely, an inversion of the Mn(II) center, from the $\Delta(ob_3)$ closed form to the $\Lambda(lel_3)$ open form, could occur during the formation of **5a**,**b** from their precursors **3a**,**b**. The central Mn atoms are four-coordinate ligated by four oxygen atoms of bridging carbohydrate residues in the $(D\text{-Man})_3$-tren ligands and one water molecule (2.19(1) Å for **5a** and 2.17(1) Å for **5b**), resulting in a square-pyramidal geometry. On the basis of the bond lengths (Tables 5 and 7), the oxidation states of the central manganese atoms are assumed to Mn(III). The C-2 and C-3 hydroxyl groups of the bridging sugar moieties are also estimated to be deprotonated from the short bond lengths to the central Mn atom (1.88(2)−1.96(2) Å for **5a** and 1.91(1)−1.93(1) Å for **5b**). The complex cations can also be viewed alternatively, namely, the two seven-coordinate Mn(II) complexes, $[Mn((D\text{-Man})_3\text{-tren})]^{2+}$, trap a Mn(III) ion through a sugar domain. To our knowledge, the present trimanganese complex is the first example of $Mn^{II}Mn^{III}Mn^{II}$ linear assemblage, whereas many $Mn^{II}Mn^{II}Mn^{II}$ and $Mn^{III}Mn^{II}$-Mn^{III} compounds have already been reported, examples being $[Mn^{II}_3(\mu\text{-OAc})_6(bpy)_2]$,[25] $[Mn^{II}_3(\mu\text{-OAc})_6(BIPhMe)_2]$ (BIPhMe = 2,2′-bis(1-methylimidazolyl)phenylmethoxymethane),[26] $[Mn^{II}_3(\mu\text{-OAc})_2(\mu\text{-bpc})_2(py)_4(H_2O)_2]$, $[Mn^{II}_3(5\text{-}NO_2\text{-salimH})_2(\mu\text{-OAc})_3]$ (5-NO_2-salimH_2 = 4-(2-((5-nitrosalicylidene)amino)ethyl)-imidazol),[18,27] $[Mn^{II}_3(\mu\text{-OAc})_2(bpc)_2(py)_4(H_2O)_2]$ (H_2bpc = 2,2′-bipyridyl-3,3′-dicarboxylic acid),[28] $[Mn^{II}_3(\mu\text{-OAc})_6(pybim)_2]$ (pybim = 2-(2-pyridyl)benzimidazole),[19] $[Mn^{III}Mn^{II}Mn^{III}(SALADHP)_2(\mu\text{-OAc})_4L_2]$ (L = MeOH, H_2O, HpyrO (= 1-aza-2-keto-3,5-cyclohexadiene), H_2SALADHP = 1,3-dihydroxy-2-methyl-2-(salicylideneamino)propane),[20−22] $[Mn^{III}Mn^{II}Mn^{III}(SALATHM)_2(\mu\text{-OAc})_4(CH_3OH)_2]$ (H_2SALATHM = tris(hydroxymethyl)(salicylideneamino)methane),[21] $[Mn^{III}Mn^{II}Mn^{III}$-

(25) Ménage, S.; Vitols, S. E.; Bergerat, P.; Codjovi, E.; Kahn, O.; Girerd, J.-J.; Guillot, M.; Solans, X.; Calvet, T. *Inorg. Chem.* **1991**, *30*, 2666.
(26) Raedin, R. L.; Poganiuch, P.; Bino, A.; Goldgerg, D. P.; Tolman, W. B.; Liu, S.; Lippard, S. J. *J. Am. Chem. Soc.* **1992**, *114*, 5240.
(27) Baldwin, M. J.; Kampf, J. W.; Pecoraro, V. L. *J. Chem. Soc., Chem. Commun.* **1993**, 1741.
(28) Zhong, Z. J.; You, X.-Z.; Mak, T. C. W. *Polyhedron* **1994**, *13*, 2157.

Chart 2

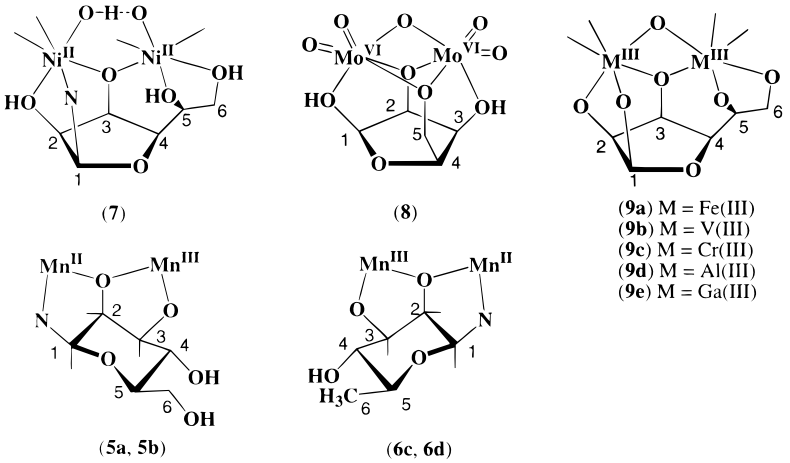

[a] Estimated standard deviations are given in parentheses.

$(HSALADHP)_2(\mu\text{-}OAc)_2(\mu\text{-}5\text{-}Cl\text{-}salicylato)_2]_n$,[23] $[Mn^{III}Mn^{II}Mn^{III}(HSALADHP)_2(\mu\text{-}OAc)_2(\mu\text{-}5\text{-}Cl\text{-}salicylato)_2(thf)]$,[19] and $[Mn^{III}Mn^{II}Mn^{III}(HB(3,5\text{-}i\text{-}Pr_2pz)_3)_2(\mu\text{-}OAc)_4(\mu\text{-}OH)_2]$.[24] Details of the bridging sugar parts are discussed in a separate chapter.

The crystal structures of $[\{Mn((L\text{-}Rha)_3\text{-}tren)\}_2Mn(H_2O)]X_3$ (**6c**, X = NO_3; **6d**, X = $^1/_2SO_4$) are isomorphous and have a crystallographically imposed C_2 symmetry with the axis passing through the Mn(1) and O(1) atoms. The structures of the complex cations are mirror images of **5a** and **5b** except the absence of C-6 hydroxyl groups of sugar units (Figure 8, Table 6). The Mn···Mn separations are 3.845(2) Å (**6c**) and 3.855(1) Å (**6d**), and the Mn···Mn···Mn angles are 173.9(1)° (**6c**) and 173.81(7)° (**6d**). The metal−metal separations are shorter by ca. 0.06 Å than those observed in **5a** and **5b** (Table 7). The structures around the terminal Mn(II) ions are almost identical to $[Mn((L\text{-}Rha)_3\text{-}tren)]SO_4$ (**4d**) with the Δ-*lel*(λ_3) configuration (Table 7). The central Mn(III) atom is four-coordinate ligated by four oxygen atoms of bridging carbohydrate residues in the $(L\text{-}Rha)_3$-tren ligands (1.890(7), 1.920(8) Å for **6c** and 1.909(4), 1.920(6) Å for **6d**) and one water molecule (2.16(1) Å for **6c** and 2.203(8) Å for **6d**) in a square-pyramidal fashion.

Structures of Bridging Carbohydrates. The structurally characterized examples with bridging carbohydrates on a dimetal center are extremely rare, since isolation and characterization of such discrete molecules were very difficult due to polymerization and hygroscopic properties. We have already reported a dinuclear Ni(II) complex with diamine tethered D-mannose, $[Ni_2(N,N'\text{-}(D\text{-}Man)_2\text{-}N,N'\text{-}Me_2en)(N\text{-}(D\text{-}Man)\text{-}N,N'\text{-}Me_2en)(CH_3OH)]Cl_2$ (**7**),[29] in which a β-D-mannosyl amine moiety takes a furanose structure and join two metals with all-cis donors, in particular, the C-3 alkoxo group acting as a monoatom bridge (Chart 2). The Ni···Ni separation is 3.596(4) Å. Similar bridging structures of deprotonated D-mannofuranose have been reported in homoleptic trivalent dimetal complexes, $Ba_2[M^{III}_2(\beta\text{-}D\text{-}mannose^{5-})_2]$ (**9**) (M = Fe, V, Cr, Al, Ga), with metal−metal distances being 3.095(2) (M = Al) to 3.298(2) Å (M = Fe) (Chart 2).[30] The all-cis bridging mode of furanose has also been observed in $[Mo^{VI}_2O_4(\mu\text{-}O)(D\text{-}lyxose^{2-})]$ (**8**),[31] where C-2 and C-5 hydroxyl groups are doubly deprotonated and both act as μ-alkoxo bridges (Chart 2). In the present complexes **5** and **6**, a β-mannopyranosyl skeletal unit with a chair conformation bridges between the two manganese ions with the C-2 μ-alkoxo group playing a key function and the C-1 N-glycosidic amino and the C-3 alkoxo groups coordinating to each metal center (Figure 9, Chart 2, Table 7). In other words, these bridging structures could be recognized as a new general equatorial−axial−equatorial (*eq*−*ax*−*eq*) bridging system with a six-membered pyranose ring. The C-2 μ-alkoxo bridging is rather asymmetric, with short bond lengths to the Mn(III) ions (1.89−1.92 Å) and long ones to the Mn(II) center (2.248−2.31 Å).

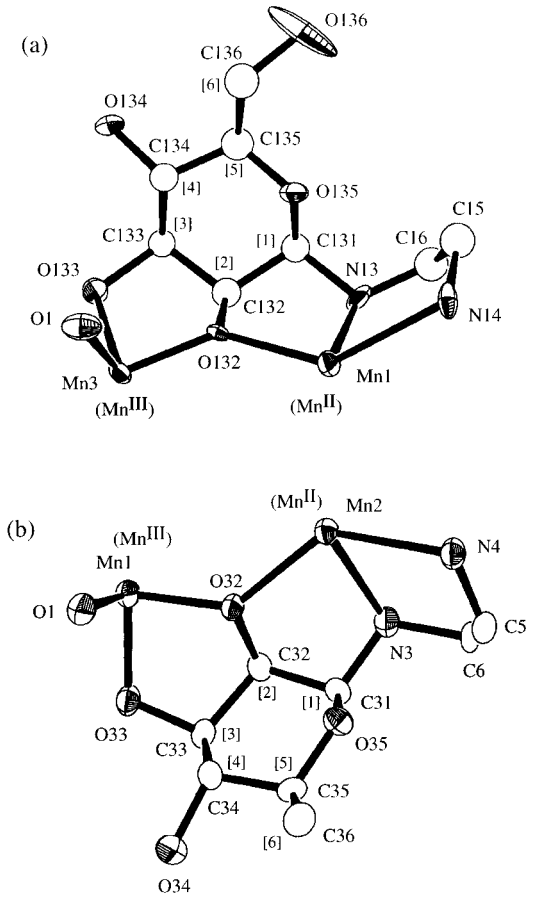

Figure 9. Perspective views for the carbohydrate bridging parts of (a) $[\{Mn((D\text{-}Man)_3\text{-}tren)\}_2Mn(H_2O)]Br_3$ (**5b**) and (b) $[\{Mn((L\text{-}Rha)_3\text{-}tren)\}_2Mn(H_2O)](SO_4)_{1.5}$ (**6d**).

(29) (a) Tanase, T.; Kurihara, K.; Yano, S.; Kobayashi, K.; Sakurai, T.; Yoshikawa, S. *J. Chem. Soc., Chem. Commun.* **1985**, 1562. (b) Tanase, T.; Kurihara, K.; Yano, S.; Kobayashi, K.; Sakurai, T.; Yoshikawa, S.; Hidai, M. *Inorg. Chem.* **1987**, *26*, 3134.
(30) Burger, J.; Gack, C.; Klüfers, P. *Angew. Chem., Int. Ed. Engl.* **1995**, *34*, 2647.
(31) Taylor, G. E.; Waters, J. M. *Tetrahedron Lett.* **1981**, *22*, 1277.

The Mn(II)−O_{2b}−Mn(III) angles range from 135.9° to 137.7°. The average O_{2b}−Mn(III)−O_{3b} and O_{2b}−Mn(II)-N^*_{sec} bite angles are 86.4° and 75.3°, respectively; these two five-membered chelate rings might bring about some strain in the six-membered pyranose ring. The observed C-2 alkoxo bridging mode on the dimanganese center is quite interesting in relation to the proposed mechanism of xylose isomerases which promote aldose−ketose isomerization by utilizing dimetal ions of Mg^{2+}, Mn^{2+}, and Co^{2+}.[4] In the proposed mechanism, an open-chain form aldose is fixed on the dimetal center (∼4.9 Å apart) with a C-2 alkoxo bridge, which might be considered to activate the C−H bond on the C-2 position and promote a 1,2-hydride shift, a key step leading to ketose.[4]

Conclusion

The present study reports the unprecedented mixed-valence trimanganese(II,III,II) complexes with the *N*-glycoside ligands $(aldose)_3$-tren, which could be derived from seven-coordinate monomanganese(II) complexes presumably through an encapsulation of an additional manganese ion by their sugar domain. The observed bridging system of β-mannopyranosyl with a C-2 μ-alkoxo group is the first structurally characterized example and could provide important structural information with relevance to sugar-metabolizing metalloenzymes such as xylose isomerases.

Acknowledgment. We are grateful to Prof. Kotaro Osakada of Tokyo Institute of Technology, Profs. Isamu Kinoshita and Akio Ichimura of Osaka City University, and Prof. Wasuke Mori of Kanagawa University. T.T. also greatly thanks Prof. Stephen J. Lippard for helpful discussion. This work was partially supported by a Grant-in-Aid for Scientific Research from the Ministry of Education of Japan and grants from Iwatani, Nippon Itagarasu, Mitsubishi-Yuka, San-ei-gen, Rigaku, and Nagase Foundations.

Supporting Information Available: Tabulations of crystallographic data, positional and thermal parameters, and bond lengths and angles for all non-hydrogen atoms for **3b**·3.5H_2O, **4d**·4CH_3OH, **5a**·6H_2O, **5b**·8H_2O, **6c**·5H_2O, and **6d**·10H_2O and ORTEP plots of complexes **5a** and **6c**. This material is available free of charge via the Internet at http://pubs.acs.org.

IC990349R